

FILE COPY

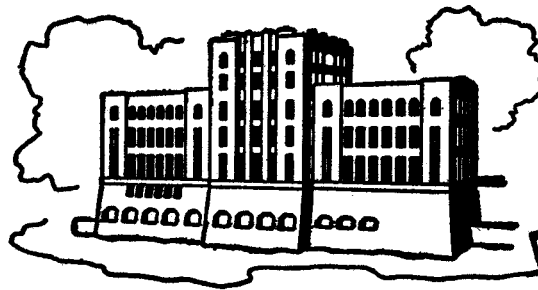
ICE FORCES ON TWO-DIMENSIONAL SLOPING STRUCTURES

by

J. S. Yean, J. C. Tatinclaux, and A. G. Cook

Sponsored by

National Science Foundation
Grant CME-77-12176-AO1
and Office of Naval Research



PLEASE DO NOT REMOVE

IIHR Report No. 230

Iowa Institute of Hydraulic Research
The University of Iowa
Iowa City, Iowa 52242

June 1981

Approved for public release; distribution unlimited

ICE FORCES ON TWO-DIMENSIONAL SLOPING STRUCTURES

by

J. S. Yean, J. C. Tatinclaux, and A. G. Cook

Sponsored by

National Science Foundation
Grant CME-77-12176-AO1
and Office of Naval Research

IIHR Report No. 230

Iowa Institute of Hydraulic Research
The University of Iowa
Iowa City, Iowa 52242

June 1981

Approved for public release; distribution unlimited

Unclassified

SECURITY CLASSIFICATION OF THIS PAGE (When Data Entered)

REPORT DOCUMENTATION PAGE		READ INSTRUCTIONS BEFORE COMPLETING FORM
1. REPORT NUMBER IIHR Report No. 230	2. GOVT ACCESSION NO.	3. RECIPIENT'S CATALOG NUMBER
4. TITLE (and Subtitle) Ice Forces on Two-Dimensional Sloping Structures		5. TYPE OF REPORT & PERIOD COVERED Technical Report
		6. PERFORMING ORG. REPORT NUMBER IIHR Report No. 230
7. AUTHOR(s) Y.S. Yean, J.C. Tatinclaux and A.G. Cook		8. CONTRACT OR GRANT NUMBER(s) N00014-79-C-0411
9. PERFORMING ORGANIZATION NAME AND ADDRESS Institute of Hydraulic Research The University of Iowa Iowa City, Iowa 52242		10. PROGRAM ELEMENT, PROJECT, TASK AREA & WORK UNIT NUMBERS
11. CONTROLLING OFFICE NAME AND ADDRESS Office of Naval Research Arlington, Virginia 22217		12. REPORT DATE June 1981
		13. NUMBER OF PAGES
14. MONITORING AGENCY NAME & ADDRESS (if different from Controlling Office)		15. SECURITY CLASS. (of this report) Unclassified
		15a. DECLASSIFICATION/DOWNGRADING SCHEDULE N/A
16. DISTRIBUTION STATEMENT (of this Report) Approved for public release, distribution unlimited		
17. DISTRIBUTION STATEMENT (of the abstract entered in Block 20, if different from Report)		
18. SUPPLEMENTARY NOTES		
19. KEY WORDS (Continue on reverse side if necessary and identify by block number) Ice forces, structures, two-dimensional, sloping		
20. ABSTRACT (Continue on reverse side if necessary and identify by block number) Analytical expressions for the horizontal and vertical forces exerted by a floating ice sheet against a two-dimensional sloping structure are derived under the assumption that ice is an elastic, homogeneous material. The specific conditions investigated are 1. Quasi-steady form of the governing equation. a. The free end of the semi-infinite ice sheet is subjected to a horizontal force, a vertical force,		

DD FORM 1 JAN 73 1473

EDITION OF 1 NOV 65 IS OBSOLETE
S/N 0102-LF-014-6601

Unclassified

SECURITY CLASSIFICATION OF THIS PAGE (When Data Entered)

and a bending moment. Failure of the ice sheet occurs before its free edge becomes fully emerged from or submerged into the water.

- b. The free end of a semi-infinite ice sheet is subjected only to a vertical force, but failure occurs after the free end has fully emerged from or submerged into the water.
- c. Finite ice sheet subjected only to a vertical force at one free end which remains at the water surface until failure occurs.

2. Unsteady form of the governing equation for a semi-infinite sheet subjected to only a vertical force at its free end which remains at the water surface until failure occurs.

It appears that, for practical applications, the effect of the horizontal force and bending moment at the free end of the ice sheet on the sheet deformation is negligible. It is shown that a finite ice sheet of length at least three times a characteristic length expressed in terms of the ice mechanical properties can be treated as a semi-infinite ice sheet. Also it is shown that when the ice thickness is smaller than a critical value which depends upon the ice mechanical properties and the direction (upward or downward) of the vertical force exerted at the sheet free end, the failure force of the ice sheet is independent of the ice elastic modulus.

The analytical results have been verified experimentally, and used in the experimental determination of the bending strength and strain modulus of urea-doped ice.

ABSTRACT

Analytical expressions for the horizontal and vertical forces exerted by a floating ice sheet against a two-dimensional sloping structure are derived under the assumption that ice is an elastic, homogeneous material. The specific conditions investigated are

1. Quasi-steady form of the governing equation.
 - a. The free end of the semi-infinite ice sheet is subjected to a horizontal force, a vertical force, and a bending moment. Failure of the ice sheet occurs before its free edge becomes fully emerged from or submerged into the water.
 - b. The free end of a semi-infinite ice sheet is subjected only to a vertical force, but failure occurs after the free end has fully emerged from or submerged into the water.
 - c. Finite ice sheet subjected only to a vertical force at one free end which remains at the water surface until failure occurs.

2. Unsteady form of the governing equation for a semi-infinite sheet subjected to only a vertical force at its free end which remains at the water surface until failure occurs.

It appears that, for practical applications, the effect of the horizontal force and bending moment at the free end of the ice sheet on the sheet deformation is negligible. It is shown that a finite ice sheet of length at least three times a characteristic length expressed in terms of the ice mechanical properties can be treated as a semi-infinite ice sheet. Also it is shown that when the ice thickness is smaller than a critical value which depends upon the ice mechanical properties and the direction (upward or downward) of the vertical force exerted at the sheet free end, the failure force of the ice sheet is independent of the ice elastic modulus.

The analytical results have been verified experimentally, and used in the experimental determination of the bending strength and strain modulus of urea-doped ice.

ACKNOWLEDGEMENTS

The present report is a revised and expanded version of the M.S. thesis by the first author under the supervision of the second author. The third author conducted the experiments on urea-doped ice.

The research reported herein was supported by the National Science Foundation under Grant No. CME 77-12176-A01, and by the Office of Naval Research.

TABLE OF CONTENTS

LIST OF FIGURES	vii
LIST OF TABLES	viii
LIST OF SYMBOLS	ix
CHAPTER	
I INTRODUCTION	1
II STATEMENT OF PROBLEM	2
III PROBLEM ANALYSIS	5
A. Governing Equations	5
1. Ice Sheet in Contact with Water Along its Whole Length	5
2. Partially Emerged Ice Sheet	8
3. Final Remarks	10
B. Initial and Boundary Conditions	10
1. Initial Conditions	10
2. Boundary Conditions	10
C. Problem Classification	12
IV SOLUTION OF THE QUASI-STEADY EQUATION	14
A. Ice Sheet in Contact with Water Along its Whole Length	14
1. General Case ($F, P, M_o \neq 0$)	14
2. Particular Conditions ($P = M_o = 0, F \neq 0$)	18
3. Examples of Application	19
B. Partially Emerged or Submerged Ice Sheet ($P, M_o = 0, F \neq 0$)	21
C. Finite Ice Sheet ($P = M_o = 0, F \neq 0$)	29
D. Discussion	32
V SOLUTIONS OF THE UNSTEADY EQUATION ($M_o = P = 0, F \neq 0$)	37
VI EXPERIMENTAL VERIFICATION AND APPLICATION	44
A. Preliminary Considerations	44
B. Methods of Calculation of σ_b and E	45
1. The y-F Method	47
2. The x-y Method	48
3. The x-F Method	48
C. Initial Experiments with Freshwater Ice Sheets	49
1. Experimental Apparatus and Procedures	49
2. Experimental Results	51

	D. Experiments with Sloping Planes	53
	E. Experimental Determination of σ_b and E for Urea-doped Ice	56
VII	SUMMARY AND CONCLUSIONS	65
VIII	REFERENCES	67

LIST OF FIGURES

Figure

1.	General Definition Sketch	3
2a.	Force Analysis of an Elementary Slice of Ice Sheet	6
2b.	Free Body Diagram of an Ice Sheet with Lifting Edge Out of Water	9
3.	Problem Classification	15
4.	Examples of Bending Moment Distribution along Semi-Infinite Ice Sheet. a) $\bar{x}_O = 0.6$; b) $\bar{x}_O = 1.4$	24
5.	Maximum Bending Strength and Its Location \bar{x}_f as a Function of \bar{x}_O	26
6.	Plot of F^* and \bar{x}_O versus y_O/H	36
7.	Plot of F^O versus σ^O with E/σ_b as Parameter	38
8.	Plot of F^O versus E/σ_b with σ^O as Parameter	39
9.	Sketch of Experimental Lift-Push Apparatus	50
10.	Sketch of Experimental Sloping Plane	54
11.	Photographs of Experimental Sloping Plane	55
12.	Photograph of Direct Drive Lift-Push Apparatus	59

LIST OF TABLES

Table

1	Comparison between Finite and Semi-Infinite Ice Sheets	33
2	Calculation of Ice Mechanical Properties - Initial Experiments with Freshwater Ice	52
3	Results of Experiments with Sloping Plane	57
4	Results of Experiments with Urea-Doped Ice	61

LIST OF SYMBOLS

a_1, a_2, a_3, a_4	coefficients
b	width of ice sheet
B	buoyancy force
c_0, c_1, c_2, c_3	coefficients
e	distance of application of reaction force R from neutral axis
E	elastic modulus of ice
f	shear force
F	vertical force on structure
F_f	vertical force at failure
\bar{F}	$F/\gamma_w bL^2$
\bar{F}_S	Laplace transform of F
F^O	$F_f/\gamma_w bh^2$
F^*	$F_f/\gamma_w bHx_f$
g	acceleration of gravity
G	special function
h	ice thickness
\bar{h}	h/L
h_o	immersed thickness of ice
h_{min}	critical ice thickness defined by equation 53a
h_{max}	critical ice thickness defined by equation 40a
H	h_o or $(h - h_o)$
\bar{H}	H/L
I	moment of inertia of ice sheet cross section
J_n	Bessel function of the first kind of order n
k_1, k_2, k_3, k_4	coefficients

ℓ	length of ice sheet
L	characteristic length of ice = $(Eh^3/3\gamma_w)^{\frac{1}{4}}$
M	bending moment
\bar{M}	$M/\gamma_w bL^3$
M_O	bending moment at edge of ice sheet
M_f	bending moment at failing section
M_S	Laplace transform of M
N	force component normal to structure
P	horizontal force on structure
P_f	horizontal force at failure
r	radius of curvature of neutral axis
R	reaction force = $\sqrt{F^2 + P^2} = \sqrt{N^2 + T^2}$
s	variable in Laplace transform
t	time
\bar{t}	t/T
T	characteristic time, also force component tangential to structure
u_O	rate of vertical displacement of ice edge
v_O	horizontal velocity of ice sheet
W	weight of ice
x	horizontal coordinate
\bar{x}	x/L
x_f	length of broken floe
x_O	length of ice totally submerged or emerged
x_S	$\bar{x}(1+s^2)^{\frac{1}{4}}$
y	vertical coordinate

\bar{y}	y/L
y_o	vertical displacement of ice sheet edge
y'_o	displacement of free edge of finite ice sheet
y_s	Laplace transform of \bar{y}
α	H/h
γ_w	specific weight of ice
Γ	gamma function
λ_1, λ_2	coefficients
μ	dynamic friction coefficient between ice and structure
ϕ	ratio P/F
ρ_i	density of ice
ρ_w	density of water
σ_b	bending strength of ice
σ_c	compressive strength of ice
σ_t	tensile stress
σ^o	$\sigma_b/\gamma_w h$
θ	angle of inclination of structure

I. INTRODUCTION

Man made structures erected in the high latitude regions of the globe must be built so as to withstand the large forces exerted by the ice which they may come in contact with. These structures may be stationary, bridge piers, warves, dykes, light houses, drilling islands etc., or mobile, tugs, icebreakers etc. The ice these structures may have to interact with can be monolithic sheets or broken ice masses either unconsolidated, ice rubble, or partially or totally refrozen, ice ridges. Since the mechanical properties of monolithic ice show its bending strength to be about half its crushing strength (e.g., Pounder 1965), ice thrust on structures can be reduced by inclining the face of the structure to force the ice to fail by bending.

Because of its importance it is not surprising that numerous studies have been devoted to the problem of ice forces on inclined structures, and related topics by an analytical approach, experimental simulation and combinations of both. For example, Nevel (1979) and Sorensen (1978) have followed the analytical route, while Tryde (1972), Ralston (1979) Frederking (1979), among others, have followed an empirio-analytical approach. Most of these researchers have treated the case of a three-dimensional structure interacting with an infinite floating ice sheet, where three-dimensional effects occur, and for which the analysis becomes extremely complicated, even when only quasi steady conditions are considered. The problem treated herein is that of a free-floating ice sheet pushing against a two-dimensional inclined plane. The problem is tractable mathematically, and it is believed that the results obtained can give better insight into the general phenomenon of ice forces on structures of more complicated shape. In particular it is shown that the relationship between the maximum force exerted by an ice sheet on an inclined plane and the ice properties, bending strength and elastic modulus, depends on whether the ice sheet is lifted out of the water or pushed down into it, or whether failure of the ice sheet occurs before or after its frontal edge becomes fully emerged from or submerged into the water, and also on how high the frontal edge emerges or how deep it submerges before failure occurs.

II. STATEMENT OF PROBLEM

The problem to be considered is that of an ice sheet floating at the surface of a body of water and which, under the influence of external forces, such as wind shear, is climbing up or down a sloping structure. Only the two-dimensional problem is considered here. The ice sheet of uniform thickness h , and width b is assumed to be homogeneous and to behave as an elastic material characterized by a modulus of elasticity E , a bending strength σ_b and a compression strength σ_c .

The chosen system of coordinates has its origin on the line of intersection between the water surface and the end of the ice sheet. The x-axis is horizontal in the plane of the water surface in the opposite direction of motion of the ice; the y-axis is vertical upward (see Figure 1). The origin of time is chosen as the instant when the ice strikes the inclined structure. The horizontal displacement velocity of the ice, V_0 , will be assumed to remain constant throughout the process.

For time $t \leq 0$, the buoyancy force balances the ice weight, such that the immersed depth of ice, h_0 , is given by

$$h_0 = \frac{\rho_i}{\rho_w} h \quad (1)$$

where ρ_i and ρ_w are the densities of ice and water, respectively.

For time $t > 0$, as the ice climbs up the structure, it is subjected to a reaction force R of components N and T in the normal and tangential directions, respectively, relative to the structure, and of components P and F in the xy -system of coordinates (see Figure 1), such that

$$F = N \cos \theta - T \sin \theta \quad (2)$$

$$P = N \sin \theta + T \cos \theta$$

where θ is the angle of inclination of the structure with respect to the horizontal plane.

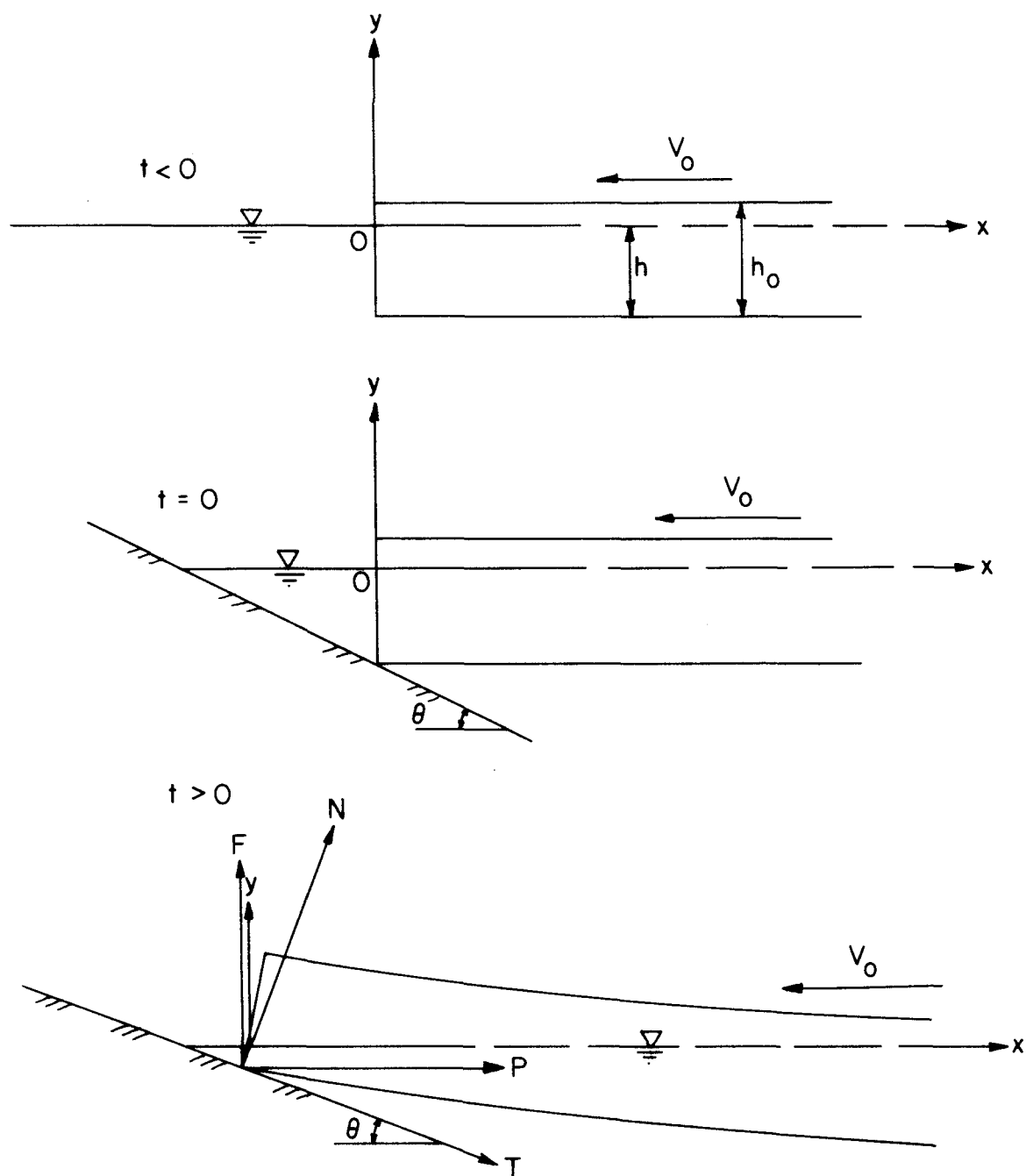


Figure 1. General Definition Sketch

When the dynamic friction coefficient, μ , at the ice-structure interface is introduced then

$$T = \mu N$$

and

$$P = \frac{\sin\theta + \mu\cos\theta}{\cos\theta - \mu\sin\theta} \quad F = \phi F \quad (3)$$

The reaction force R acts at the point of contact of the ice sheet with the structure.

Under the action of F and P , the ice sheet undergoes a displacement $y(x,t)$ from its initial free floating position, and is subjected to a moment distribution $M(x,t)$. The ice sheet will fail at a distance x_f from the upstream end, where the stress at the top or bottom of the ice sheet reaches either the bending strength, σ_b , or the compressive strength, σ_c , of the ice. However, since the tensile strength of ice is approximately half its compressive strength (see, for example, Pounder 1965, Weeks and Assur 1969), it will be assumed that the ice sheet will fail in tension. The distance of failure x_f is then determined by

$$\sigma_b = \frac{M_f h}{2I} - \frac{P}{bh} \quad (4)$$

or

$$\sigma_b = \frac{M_f h}{2I} - \frac{\phi F}{bh} \quad (4a)$$

where $M_f = M(x_f, t)$ and $I = \frac{bh^3}{12}$ is the moment of inertia of the beam cross-section about the neutral axis.

III. PROBLEM ANALYSIS

A. Governing Equations

1. Ice Sheet in Contact with Water Along its Whole Length

Consider an elementary slice of the ice sheet of length dx as shown in figure 2a. The ice element is displaced by the distance y from its free floating position, and is subjected to the various forces and moments indicated on figure 2a. Application of Newton's second law in the y -direction leads to

$$(\rho_i b h dx) \frac{\partial^2 y}{\partial t^2} = f + dB - dW - (f + \frac{\partial f}{\partial x} dx) \quad (5)$$

where f = shear force

$$dB = \text{buoyancy force on ice element} = \gamma_w (h_o - y) b dx$$

$$dW = \text{weight of ice element} = \gamma_i h dx = \gamma_w \frac{h}{h_o} b dx$$

Equation 5 gives

$$\frac{\partial f}{\partial x} = -\gamma_w \frac{b h}{h_o} \left(\frac{y}{h_o} + \frac{1}{g} \frac{\partial^2 y}{\partial t^2} \right) \quad (6)$$

The shear force distribution along the ice sheet is then given by

$$f(x,t) = F + \int_0^x \frac{\partial f}{\partial x} dx \quad (7)$$

The transverse deformation $y(x,t)$ of the ice sheet is related to the moment $M(x,t)$ exerted at any section by

$$\frac{M(x,t)}{EI} = \frac{1}{r} = \frac{\partial^2 y / \partial x^2}{\left[1 + \left(\frac{\partial y}{\partial x} \right)^2 \right]^{3/2}} \quad (8)$$

where r is the radius of curvature of the neutral axis. When it is assumed that the transverse deformation is small enough for $(\partial y / \partial x)^2$ to be negligible with respect to 1, equation 8 reduces to

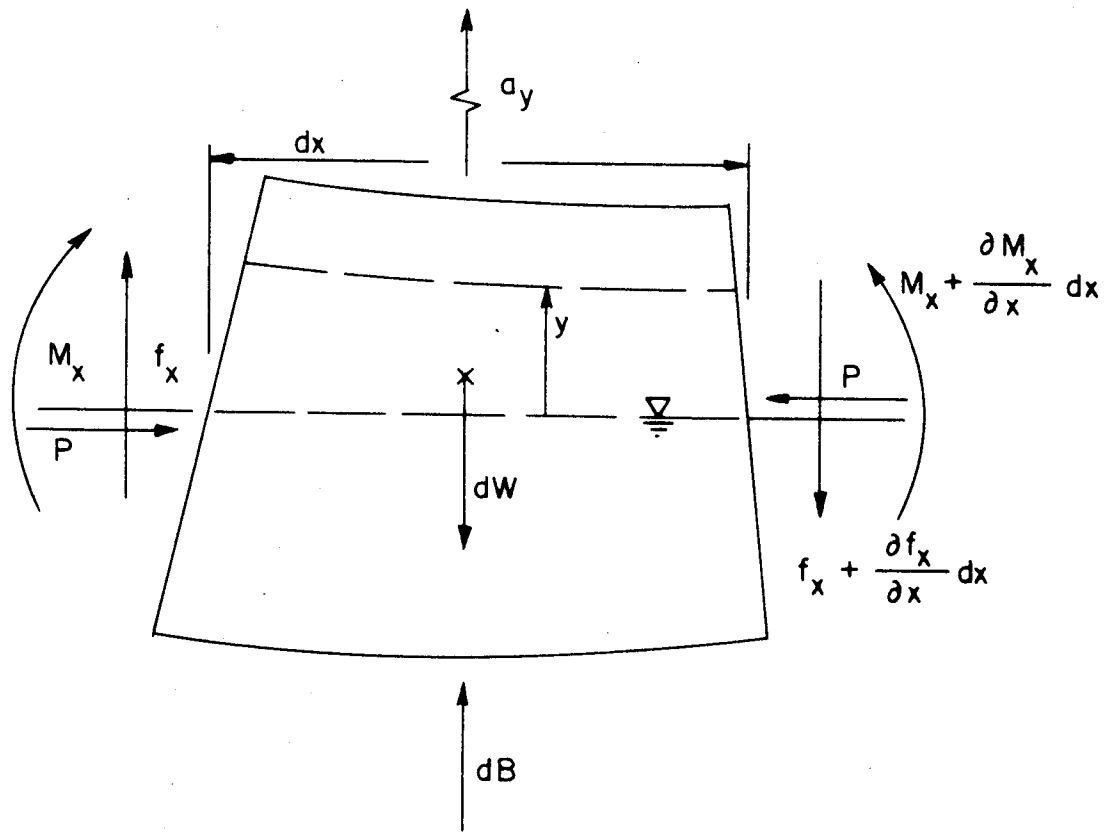


Figure 2a. Force Analysis of an Elementary Slice of Ice Sheet

$$\frac{M}{EI} = \frac{\partial^2 y}{\partial x^2} \quad (9)$$

The reactions F and P exerted at the bottom of the free end in contact with the structure can be replaced by the same two forces exerted at the neutral axis of the ice sheet plus a bending moment M_0 , as shown in Figure 1. When moment equilibrium is applied to a sheet element of length dx , or to a segment of ice sheet extending from the free end to a distance x , the following relationship for the bending moment exerted at any section x of the ice sheet is obtained

$$M(x,t) = M_0 + P(y_0 - y) + \int_0^x f \, dx \quad (10)$$

where y_0 is the vertical displacement of the free end from its free floating position. When equation 10 is differentiated twice with respect to x , it yields

$$\frac{\partial^2 M}{\partial x^2} = -P \frac{\partial^2 y}{\partial x^2} + \frac{\partial f}{\partial x} \quad (11)$$

When equations 4, 5 and 9 are substituted into equation 11, the governing equation for the deformation $y(x,t)$ is obtained as

$$\frac{\partial^4 y}{\partial x^4} + \frac{\phi F}{EI} \frac{\partial^2 y}{\partial x^2} + \frac{\gamma_w b}{EI} \left(y + \frac{h_0}{g} \frac{\partial^2 y}{\partial t^2} \right) = 0 \quad (12)$$

The following dimensionless variables are introduced

$$\bar{y} = y/L, \quad \bar{x} = x/L, \quad \bar{t} = t/T, \quad \bar{F} = F/\gamma_w bL^2$$

$$\bar{M} = M/\gamma_w bL^3$$

where L is a characteristic length defined by

$$L = \left(\frac{4EI}{\gamma_w b} \right)^{\frac{1}{4}} = \left(\frac{Eh^3}{3\gamma_w} \right)^{\frac{1}{4}} \quad (13)$$

and T is a characteristic time defined by

$$T = (h_o/g)^{\frac{1}{2}} \quad (14)$$

Then the dimensionless governing equation is:

$$\frac{\partial^4 \bar{y}}{\partial \bar{x}^4} + 4\phi \bar{F} \frac{\partial^2 \bar{y}}{\partial \bar{x}^2} + 4(\bar{y} + \frac{\partial^2 \bar{y}}{\partial \bar{t}^2}) = 0 \quad (15)$$

2. Partially Emerged Ice Sheet

The above derivation and the resulting governing equation 15 are valid only as long as the ice sheet at any point along its length is neither fully emerged from nor fully submerged into the water, i.e., for

$$-(h-h_o) < y(x,t) < h_o$$

In particular, if the free end emerges from the water prior to failure, the above analysis needs to be modified over the emerged length x_o as shown in Figure 2b. Newton's second law applied to an elementary ice element dx in the region $x < x_o$ yields

$$(\rho_i b h \, dx) \frac{\partial^2 y}{\partial t^2} = f - dW - (f + \frac{\partial f}{\partial x}) \, dx \quad (5a)$$

or

$$\frac{\partial f}{\partial x} = -\gamma_w b h_o (1 + \frac{1}{g} \frac{\partial^2 y}{\partial t^2}) \quad (6a)$$

Equations 10 and 11 remain valid over $0 < x < x_o$, therefore the governing equation for the displacement $y(x,t)$ over the emerged length of ice sheet becomes

$$\frac{\partial^4 y}{\partial x^4} + \frac{\phi F}{EI} \frac{\partial^2 y}{\partial x^2} + \frac{\gamma_w b h_o}{EI} (1 + \frac{1}{g} \frac{\partial^2 y}{\partial t^2}) = 0 \quad (12a)$$

or, in dimensionless form,

$$\frac{\partial^4 \bar{y}}{\partial \bar{x}^4} + 4\phi \bar{F} \frac{\partial^2 \bar{y}}{\partial \bar{x}^2} + 4(\bar{h}_o + \frac{\partial^2 \bar{y}}{\partial \bar{t}^2}) = 0 \quad (15a)$$

where $\bar{h}_o = h_o/L$ and, valid for $0 \leq \bar{x} \leq \bar{x}_o$

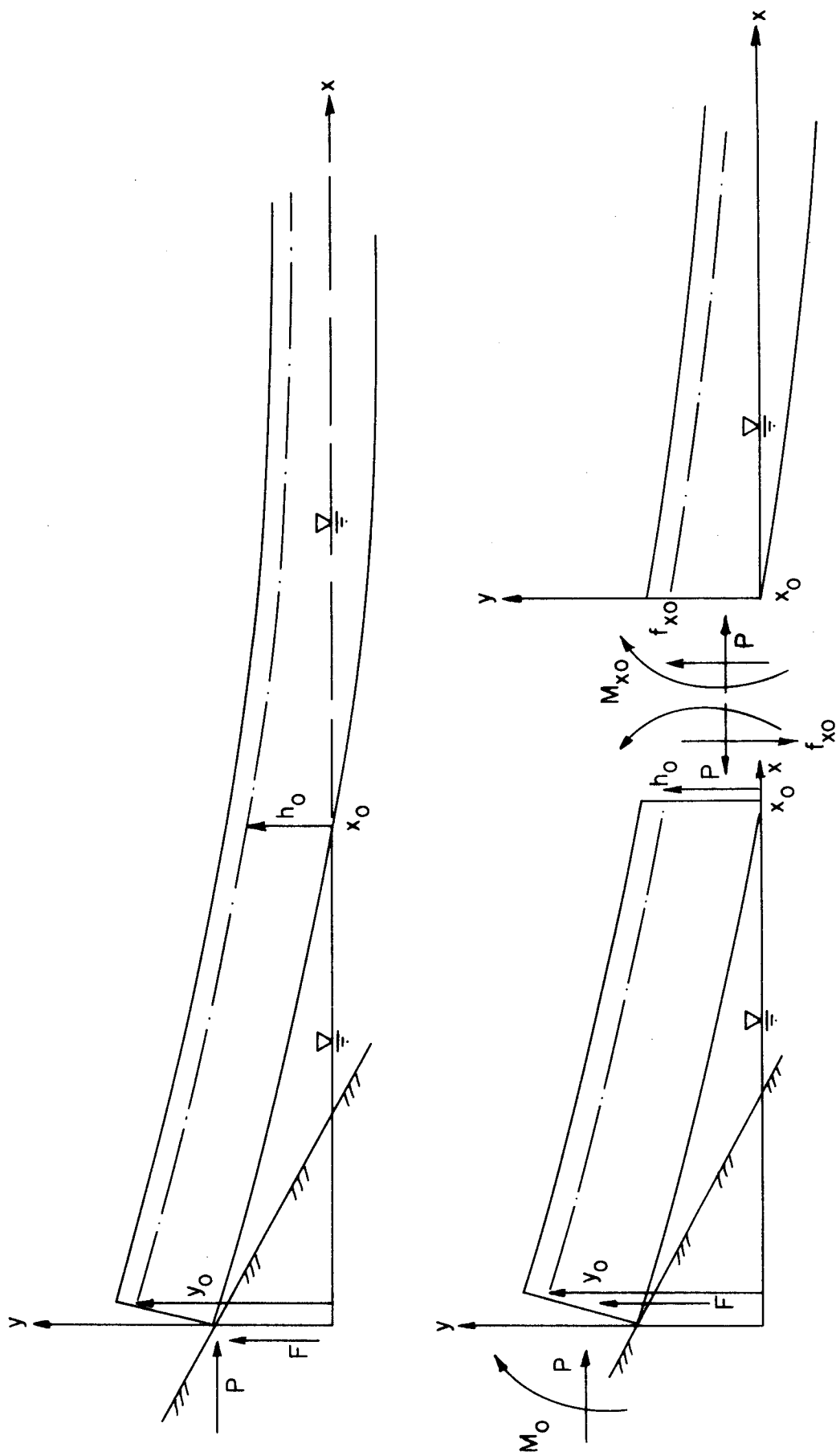


Figure 2b. Free Body Diagram of an Ice Sheet with Lifting Edge Out of Water

Equations 12 and 15 remain valid for $x > x_0$, i.e., $\bar{x} > \bar{x}_0$.

3. Final Remarks

In the derivation of Equations 15 and 15a it was implicitly assumed that the vertical force F exerted at the free end of the ice sheet was directed upward. If, on the contrary, F is directed downward, these equations are still valid provided that the displacement \bar{y} (\bar{x}, \bar{t}) be taken positive downward and that \bar{h}_0 be replaced by $(\bar{h} - \bar{h}_0)$ in Equation 15a. In summary, the dimensionless governing equations are:

$$\frac{\partial^4 \bar{y}}{\partial \bar{x}^4} + 4 \phi \bar{F} \frac{\partial^2 \bar{y}}{\partial \bar{x}^2} + 4(\bar{y} + \frac{\partial^2 \bar{y}}{\partial \bar{t}^2}) = 0 \quad (15)$$

for $\bar{y} < \bar{H}$

$$\frac{\partial^4 \bar{y}}{\partial \bar{x}^4} + 4 \phi \bar{F} \frac{\partial^2 \bar{y}}{\partial \bar{x}^2} + 4(\bar{H} + \frac{\partial^2 \bar{y}}{\partial \bar{t}^2}) = 0 \quad (16)$$

for $\bar{y} > \bar{H}$

where $\bar{H} = \bar{h}_0$ if ice sheet subjected to a lift force,

$\bar{H} = \bar{h} - \bar{h}_0$ if ice sheet subjected to a downward push

B. Initial and Boundary Conditions

1. Initial Conditions

When the unsteady form of the governing equations are considered, the initial condition is simply $\bar{y}(\bar{x}, 0) = 0$.

2. Boundary Conditions

There are three possible boundaries to be considered; the upstream edge of the ice sheet, $x = 0$, which is in contact with the structure and is submitted to the forces F and P , and a moment M_0 ; the downstream end of the sheet corresponding to $x = \infty$ for a semi-infinite sheet, and to $x = \ell$ for a sheet of finite length ℓ ; and finally, in the case of a partially emerged (or submerged) sheet, the location $x = x_0$

a) at $x = 0$ the boundary conditions are

$$\bar{y} = \bar{y}_0 = \bar{u}_0 \bar{t} \quad (17)$$

$$\frac{\partial^2 \bar{y}}{\partial \bar{x}^2} = 4 \bar{M}_0 \quad (18)$$

$$\frac{\partial^3 \bar{y}}{\partial \bar{x}^3} + 4 \phi \bar{F} \frac{\partial \bar{y}}{\partial \bar{x}} = 4 \bar{F} \quad (19)$$

where \bar{u}_0 is the dimensionless constant vertical velocity of motion of ice edge in contact with the structure

b) at $x \rightarrow \infty$ for a semi-infinite ice sheet

$$\frac{\partial^n \bar{y}}{\partial \bar{x}^n} \rightarrow 0 \quad n = 0, 1, 2, \dots \quad (20)$$

c) at $x = \ell$ for a sheet of finite length

$$\bar{M}(x = \ell) = 0 \text{ or } \left. \frac{\partial^2 \bar{y}}{\partial \bar{x}^2} \right|_{\bar{x}=\ell} = 0 \quad (21)$$

d) at $x = x_0$, for the case of an ice sheet totally emerged, or submerged, over a length x_0 . Let $\bar{y}_1(\bar{x}, \bar{t})$ be the solution of Equation (16), valid for $\bar{x} < \bar{x}_0$, and $\bar{y}_2(\bar{x}, \bar{t})$ the solution of Equation 15, valid for $\bar{x} > \bar{x}_0$. We shall require continuity of displacement, slope, moment and shear, at $x = x_0$ namely

$$\bar{y}_1 = \bar{y}_2 = \bar{H} \quad (22a)$$

$$\frac{\partial \bar{y}_1}{\partial \bar{x}} = \frac{\partial \bar{y}_2}{\partial \bar{x}} \quad (22b)$$

$$\frac{\partial^2 \bar{y}_1}{\partial \bar{x}^2} = \frac{\partial^2 \bar{y}_2}{\partial \bar{x}^2} \quad (22c)$$

$$\frac{\partial^3 \bar{y}_1}{\partial \bar{x}^3} = \frac{\partial^3 \bar{y}_2}{\partial \bar{x}^3} \quad (22d)$$

all at $\bar{x} = \bar{x}_0$

Note that the boundary condition given by equation 19 expresses that the shear force f at $x = 0$ must be equal to F , and can also be used to calculate F , once the deformation function $y(x,t)$ has been determined. Note also that F can be obtained by combining Equations 7 and 8, with the condition that f is zero at the downstream end of the ice sheet, and therefore is given in dimensionless form by

$$\bar{F} = \int_0^{\bar{x}_0} \left(\bar{H} + \frac{\partial^2 \bar{y}}{\partial \bar{t}^2} \right) d\bar{x} + \int_{\bar{x}_0}^{\infty \text{ or } \bar{\ell}} \left(\bar{y} + \frac{\partial^2 \bar{y}}{\partial \bar{f}^2} \right) d\bar{x} \quad (23)$$

or

$$4\bar{F} = - \left[\frac{\partial^3 \bar{y}}{\partial \bar{x}^3} + 4 \phi \bar{F} \frac{\partial^2 \bar{y}}{\partial \bar{x}^2} \right]_{\bar{x} = \bar{\ell}} \quad (23a)$$

C. Problem Classification

The solution of the governing equation will depend upon the boundary conditions imposed, whether the motion can be assumed to be quasi-steady or not. The various problems are schematically represented in Figure 3.

The problems treated in the following sections are

1. Quasi steady deformation of a semi-infinite ice sheet for the case $y_0 < H$ and for

- a. F , P and M_0 all different from zero
- b. Only F different from zero.

2. Semi-infinite ice sheet in quasi-steady deformation, partially emerged or submerged ($y_0 > H$), with $F \neq 0$ but $P = M_0 = 0$.

3. Quasi steady deformation of a finite ice sheet for the case $y_0 < H$ and with $F \neq 0$, $P = M_0 = 0$.

4. Unsteady deformation of a semi-infinite ice sheet, such that $y_0 < H$ and with $F \neq 0$, $P = M_0 = 0$.

IV. SOLUTIONS OF THE QUASI-STEADY EQUATION

A. Semi-Infinite Ice Sheet in Contact with Water Along its Whole Length

1. General Case (F , P and $M_0 \neq 0$).

The governing equation 15 reduces to

$$\frac{d^4 \bar{y}}{d\bar{x}^4} + 4 \phi \bar{F} \frac{d^2 \bar{y}}{d\bar{x}^2} + 4 \bar{y} = 0 \quad (24)$$

and the boundary conditions are

$$\bar{y} \text{ and } \frac{d^n \bar{y}}{d\bar{x}} \rightarrow 0 \text{ as } \bar{x} \rightarrow \infty$$

$$\bar{y} = \bar{y}_0 \text{ at } \bar{x} = 0$$

$$\frac{d^2 \bar{y}}{d\bar{x}^2} = 4 \bar{M}_0 \text{ at } \bar{x} = 0$$

The solution of equation 24 which satisfies the boundary conditions are:

$$\bar{y} = e^{\lambda_1 \bar{x}} (k_1 \cos \lambda_2 \bar{x} + k_2 \sin \lambda_2 \bar{x}) \quad (25)$$

with

$$\lambda_1 = (1 - \phi \bar{F})^{\frac{1}{2}} \quad \lambda_2 = (1 + \phi \bar{F})^{\frac{1}{2}}$$

$$k_1 = \bar{y}_0 \quad k_2 = - \frac{2\bar{M}_0 + \phi \bar{F} \bar{y}_0}{\lambda_1 \lambda_2}$$

From either equation 19 or equation 23, the vertical force \bar{F} must satisfy the relation

$$\bar{F} = \frac{(1-2\phi \bar{F})\bar{y}_0 - 2\bar{M}_0}{2\sqrt{1-\phi \bar{F}}} \quad (26)$$

The bending moment distribution is given by

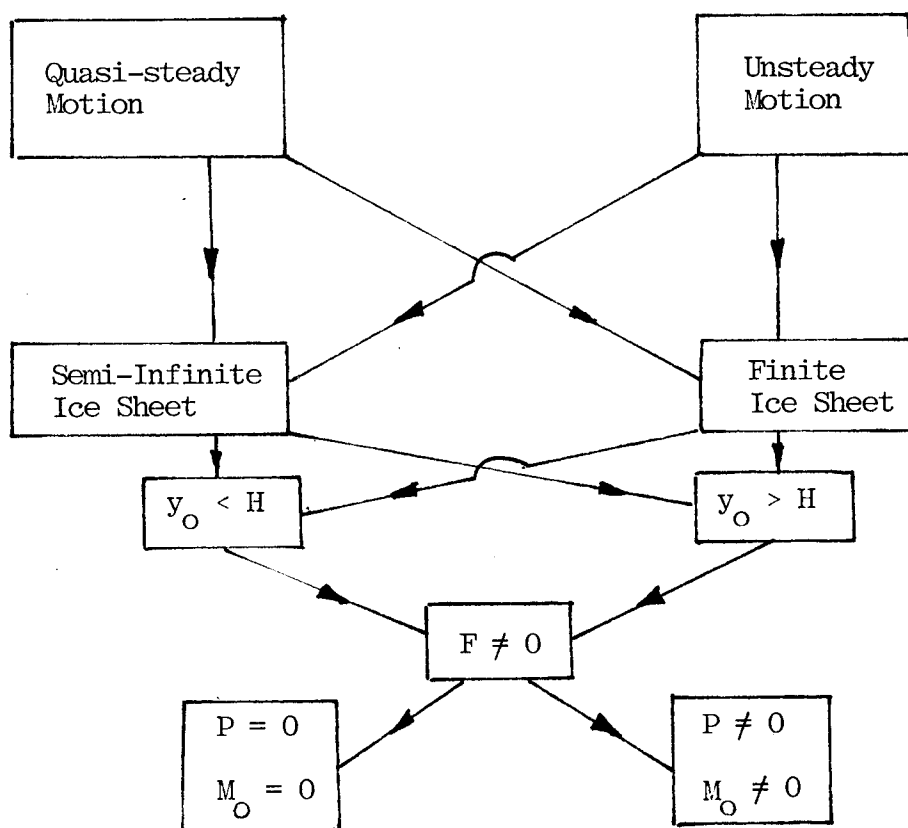


Figure 3. Problem Classification

$$\begin{aligned}
\bar{M} &= \frac{1}{4} \frac{d^2 \bar{y}}{d\bar{x}^2} \\
&= \frac{\lambda_1}{4} e^{\lambda_1 \bar{x}} \left\{ \left[(\lambda_1^2 - \lambda_2^2) k_1 - 2\lambda_1 \lambda_2 k_2 \right] \cos \lambda_2 \bar{x} \right. \\
&\quad \left. + \left[(\lambda_1^2 - \lambda_2^2) k_2 + 2\lambda_1 \lambda_2 k_1 \right] \sin \lambda_2 \bar{x} \right\} \\
&= e^{\lambda_1 \bar{x}} \left\{ \bar{M}_0 \cos \lambda_2 \bar{x} + \frac{\bar{M}_0 \phi \bar{F} + \bar{y}_0/2}{\lambda_1 \lambda_2} \sin \lambda_2 \bar{x} \right\} \quad (27)
\end{aligned}$$

The location \bar{x}_f of the maximum bending moment is obtained from $\frac{d\bar{M}}{d\bar{x}} \Big|_{\bar{x}=\bar{x}_f} = 0$ as

$$\bar{x}_f = \frac{1}{\lambda_2} \tan^{-1} \left\{ \sqrt{\frac{1+\phi\bar{F}}{1-\phi\bar{F}}} \frac{(2\phi\bar{F}-1)2\bar{M}_0 + \bar{y}_0}{(2\phi\bar{F}+1)2\bar{M}_0 + \bar{y}_0} \right\} \quad (28)$$

The tensile stress at either the top or bottom of the ice sheet at the section \bar{x}_f is given in dimensionless form by

$$\bar{\sigma}_t = 2 \bar{M}_f \bar{h} - \frac{\phi \bar{F} \bar{h}^2}{3} \quad (29)$$

and the failure criterion is

$$\bar{\sigma}_t = \bar{\sigma}_b \quad (30)$$

where

$$\bar{\sigma} = \sigma/E$$

The following procedure is suggested for determining the forces F and P exerted by an ice sheet on a two dimensional sloping structure.

1. The geometric and material characteristics of the ice sheet ($b, h, E, \sigma_b, \rho_i$), structure angle θ , and the friction coefficient μ are assumed to be known. Then the characteristic length L , time T , and coefficient ϕ , are known.

2. Assume a value for y_o and therefore $\bar{y}_o = y_o/L$.
3. Determine the corresponding value of \bar{F} by solving equation 26.
4. Determine the location \bar{x}_f of the maximum tensile stress from equation 28.
5. Calculate \bar{M}_f from equation 27 and $\bar{\sigma}_t$ from equation 29.
6. Compare $\bar{\sigma}_t$ with $\bar{\sigma}_b$;

If $\bar{\sigma}_t = \bar{\sigma}_b$ computations are stopped

If $\bar{\sigma}_t < \bar{\sigma}_b$ repeat steps 3 to 6 with a higher value of \bar{y}_o .

If $\bar{\sigma}_t > \bar{\sigma}_b$ repeat steps 3 to 6 with a smaller value of \bar{y}_o .

It should be noted that the determination of \bar{F} from equation 26, requires that \bar{M}_o be estimated. The moment M_o is related to the horizontal force P by

$$M_o = -Pe$$

where e is the distance from the point of application of the reaction force R to the neutral axis of the ice sheet, located at mid-thickness. When the ice sheet comes in contact with the structure, its leading edge will be somewhat crushed. However, the eccentricity e can be approximated by $h/2$, then

$$M_o = -\phi F h/2$$

$$\bar{M} = -\phi \bar{F} \bar{h}/2$$

with this approximation, equation 26 becomes

$$\bar{F} = \frac{(1-2\phi\bar{F})\bar{y}_o + \phi\bar{F}\bar{h}}{2\sqrt{1-\phi\bar{F}}} \quad (26a)$$

2. Particular Conditions ($F \neq 0$, $P = M_o = 0$).

For practical application, or to determine a starting value of \bar{y}_o , it may be sufficient to consider that the ice sheet is subjected only to a vertical force F . The equations derived in the previous section greatly simplify to read

$$\bar{y} = \bar{e}^{\bar{x}} \cos \bar{x} \quad (31)$$

$$\bar{F} = \frac{\bar{y}_o}{2} \quad (32)$$

$$\bar{x}_f = \tan^{-1} 1 = \frac{\pi}{4} \quad (33)$$

$$\bar{M}_f = \frac{\bar{e}^{\pi/4} \sqrt{2}}{4} \bar{y}_o = 0.161 \bar{y}_o \quad (34)$$

$$\bar{\alpha}_t = 0.322 \bar{h} \bar{y}_o \quad (35)$$

and therefore the force at failure (i.e., when $\bar{\alpha}_t = \bar{\alpha}_b$) \bar{F}_f can be obtained directly in terms of $\bar{\alpha}_b$ and \bar{h}

$$\bar{F}_f = 1.55 \frac{\bar{\alpha}_b}{\bar{h}} \quad (36)$$

while the value of \bar{y}_o at failure is given by

$$\bar{y}_{of} = 3.102 \frac{\bar{\alpha}_b}{\bar{h}} \quad (37)$$

More commonly encountered dimensionless forms of F_f , x_f and y_{of} are then given by

$$\frac{F_f}{\gamma_w b h^2} = 0.68 \left(\frac{\alpha_b}{E} \right)^{1/4} \left(\frac{\alpha_b}{\gamma_w h} \right)^{3/4} \quad (38a)$$

$$\frac{x_f}{h} = 0.60 \left(\frac{E}{\alpha_b} \right)^{1/4} \left(\frac{\alpha_b}{\gamma_w h} \right)^{1/4} \quad (38b)$$

$$\frac{y_{of}}{h} = 1.79 \left(\frac{\sigma_b}{E}\right)^{1/2} \left(\frac{\sigma_b}{\gamma_w h}\right)^{1/2} \quad (38c)$$

It is worth noting that according to equations 38, the force F_f is proportional to the bending strength σ_b and inversely proportional to the fourth root of E , only. Therefore, in model studies of ice forces on structures, proper scaling of the bending strength is more critical than that of the elastic modulus, since a 100 percent error on E leads to an error on F_f of only sixteen percent.

It is recalled that equations 38a to 38c are valid as long as the free end of the ice sheet does not either emerge from or become submerged into the water, i.e., as long as

$$\frac{y_{of}}{h} \leq \frac{H}{h} = \alpha \quad (39)$$

where α is equal to ρ_i/ρ_w when the sheet is lifted, and α equals $(1 - \frac{\rho_i}{\rho_w})$ when the sheet is pushed down. Therefore, the condition of application of equations 38a to 38c, can be expressed from equation 38c as

$$h \geq \frac{3.20}{\alpha} \frac{\sigma_b^2}{\gamma_w E} = h_{\max} \quad (40a)$$

or

$$\frac{E}{\sigma_b} \geq \frac{3.20}{\alpha} \left(\frac{\sigma_b}{\gamma_w E}\right) \quad (40b)$$

3. Example of Application

Consider an ice sheet of thickness $h = 40$ cm, with $b = 1$ m, and properties

$$\sigma_b = 1 \times 10^6 \text{ Pa}$$

$$E = 5 \times 10^9 \text{ Pa}$$

$$\rho_i = 920 \text{ kg/m}^3 \quad \rho_w = 1000 \text{ kg/m}^3$$

and climbing up an inclined structure of angle $\theta = 30^\circ$. We will assume a friction factor between the ice and the structure of $\mu = 0.15$.

It can be verified that equation 40 is satisfied. The corresponding characteristic length L and coefficient ϕ are, respectively, $L = 10.21$ m, $\phi = 0.796$.

1st Method: If the effect of the horizontal force P and moment M_O are neglected, then equations 33a to 38c are applicable and yield

$$y_{O_f} = 0.162 \text{ m}$$

$$F_f = 8100 \text{ N}$$

Failure is predicted to occur at a distance $x_f = 8.0$ m and the maximum horizontal force P_f on the structure is

$$P_f = \phi F_f = 6450 \text{ N}$$

2nd Method: When P and M_O are not neglected, but under the assumption that the excentricity e is equal to $h/2$, i.e., that $\bar{M}_O = -\phi \bar{F} \bar{h}/2$, the problem requires the simultaneous solution of equations 26, 27, and 28, varying the value of \bar{y}_O until the bending stress given by equation 29 is found equal to the ice bending strength.

With the numerical data chosen in the present example, the dimensionless values are found to be

$$\bar{y}_O = 1.635 \cdot 10^{-2}$$

$$\bar{F} = 8.225 \cdot 10^{-3}$$

$$\bar{x}_f = 8.017 \cdot 10^{-1}$$

The corresponding dimensional values are

$$y_{O_f} = 0.167 \text{ m}$$

$$F = 8400 \text{ N}$$

$$x_f = 8.19 \text{ m}$$

$$P_f = \phi F_f = 6700 \text{ N}$$

This example indicates that the effect of P and M_O on the failure force is relatively small, of the order of 5 percent in the present case, and that they may be safely neglected and still obtain a reliable estimate of the forces exerted on the structure.

B. Partially Emerged or Submerged Semi-Infinite Ice Sheet ($P = M_O = 0, F \neq 0$)

The case when the free end of the ice sheet becomes either fully emerged from or fully submerged into the water, i.e., for $y_O > H$, will be investigated only under the assumption of quasi-steady condition and of zero horizontal force and moment at the upstream edge $x = 0$. Under these assumptions the governing equations 16 and 15 reduce to

$$\frac{\partial^4 \bar{y}_1}{\partial \bar{x}^4} + 4 \bar{H} = 0 \quad 0 \leq \bar{x} \leq \bar{x}_O; \bar{y}_1 > \bar{H} \quad (41a)$$

$$\frac{\partial^4 \bar{y}_2}{\partial \bar{x}^4} + 4 \bar{y}_2 = 0 \quad \bar{x} \geq \bar{x}_O; \bar{y}_2 < \bar{H} \quad (41b)$$

where \bar{x}_O is that length of the ice sheet which is entirely either below or above water. The boundary conditions are given by equations 17 to 20 and 22a to 22d.

The solutions of equations 41a and 41b have the forms:

$$\bar{y}_1 = -\frac{\bar{H}}{6} \bar{x}^4 + C_3 \bar{x}^3 + C_2 \bar{x}^2 + C_1 \bar{x} + C_0, \quad (42a)$$

$$\bar{x} \leq \bar{x}_0$$

$$\bar{y}_2 = e^{\bar{x}'} (k_1 \cos x' + k_2 \sin x'), \quad (42b)$$

$$x' = \bar{x} - \bar{x}_0 \geq 0$$

Note that equation 42b satisfies the boundary condition given by equation 20. From the remaining boundary conditions, the coefficients k_1, k_2, C_0, C_1, C_2 and C_3 are found to be

$$k_1 = \bar{H}$$

$$k_2 = -\bar{H} \bar{x}_0$$

$$C_0 = \bar{y}_0$$

$$C_1 = -\frac{\bar{H}}{3} (2 + (1+\bar{x}_0)^3)$$

$$C_2 = 0$$

$$C_3 = \frac{1}{3} \bar{H}(1+\bar{x}_0)$$

and \bar{x}_0 is given by the relationship

$$\frac{\bar{y}_0}{\bar{H}} - \left(\frac{1}{6} \bar{x}_0^4 + \frac{2}{3} \bar{x}_0^3 + \bar{x}_0^2 + \bar{x}_0 + 1 \right) = 0 \quad (43a)$$

or

$$\frac{\bar{y}_0}{\bar{H}} = \frac{1}{6} ((1+\bar{x}_0)^4 + 2(1+\bar{x}_0) + 3) \quad (43b)$$

The force F exerted at the free end of the ice sheet is obtained from equation 23, for quasi steady conditions, as

$$\bar{F} = \int_0^{\infty} \bar{y} \, d\bar{x} = \int_0^{\bar{x}_0} \bar{H} \, d\bar{x} + \int_{\bar{x}_0}^{\infty} \bar{y}_2 \, d\bar{x}$$

$$\bar{F} = \frac{1+\bar{x}_0}{2} \bar{H} \quad (44)$$

The expressions for the bending moment \bar{M} obtained from the dimensionless form of equation 9 are given by

$$\bar{M} = \frac{\bar{H}}{2} \bar{x} (1 + \bar{x}_0 - \bar{x}) \text{ for } \bar{x} < \bar{x}_0 \quad (45a)$$

$$\bar{M} = \frac{\bar{H}}{2} (\bar{x}_0 \cos(\bar{x}-\bar{x}_0) + \sin(\bar{x}-\bar{x}_0)) e^{-(\bar{x}-\bar{x}_0)} \quad (45b)$$

for $\bar{x} > \bar{x}_0$

Failure of the ice sheet occurs when the first maximum of the bending moment satisfies

$$\bar{M}_f = \frac{\bar{\alpha}_b}{2\bar{h}} \quad (46)$$

Examination of equations 45a and 45b shows that the maximum \bar{M}_f of \bar{M} occurs at a distance \bar{x}_f less than \bar{x}_0 , i.e., in the fully emerged or submerged part of the ice sheet, when $\bar{x}_0 < 1$, but greater than \bar{x}_0 , for $\bar{x}_0 > 1$. For illustration purposes the distribution of the bending moment \bar{M}_x is shown in Figure 4 for the two particular values $\bar{x}_0 = 0.6$ and $\bar{x}_0 = 1.4$.

The location \bar{x}_f of the maximum bending moment corresponding to $(d\bar{M}_x/d\bar{x})_{\bar{x}=\bar{x}_f} = 0$ is then given by

$$\bar{x}_f = \bar{x}_0 + \tan^{-1} \left(\frac{1-\bar{x}_0}{1+\bar{x}_0} \right) = \bar{x}_0 + \frac{\pi}{4} - \tan^{-1} (\bar{x}_0), \text{ for } \bar{x}_0 < 1 \quad (47a)$$

or

$$\bar{x}_f = \frac{1+\bar{x}_0}{2} \text{ for } \bar{x}_0 > 1 \quad (47b)$$

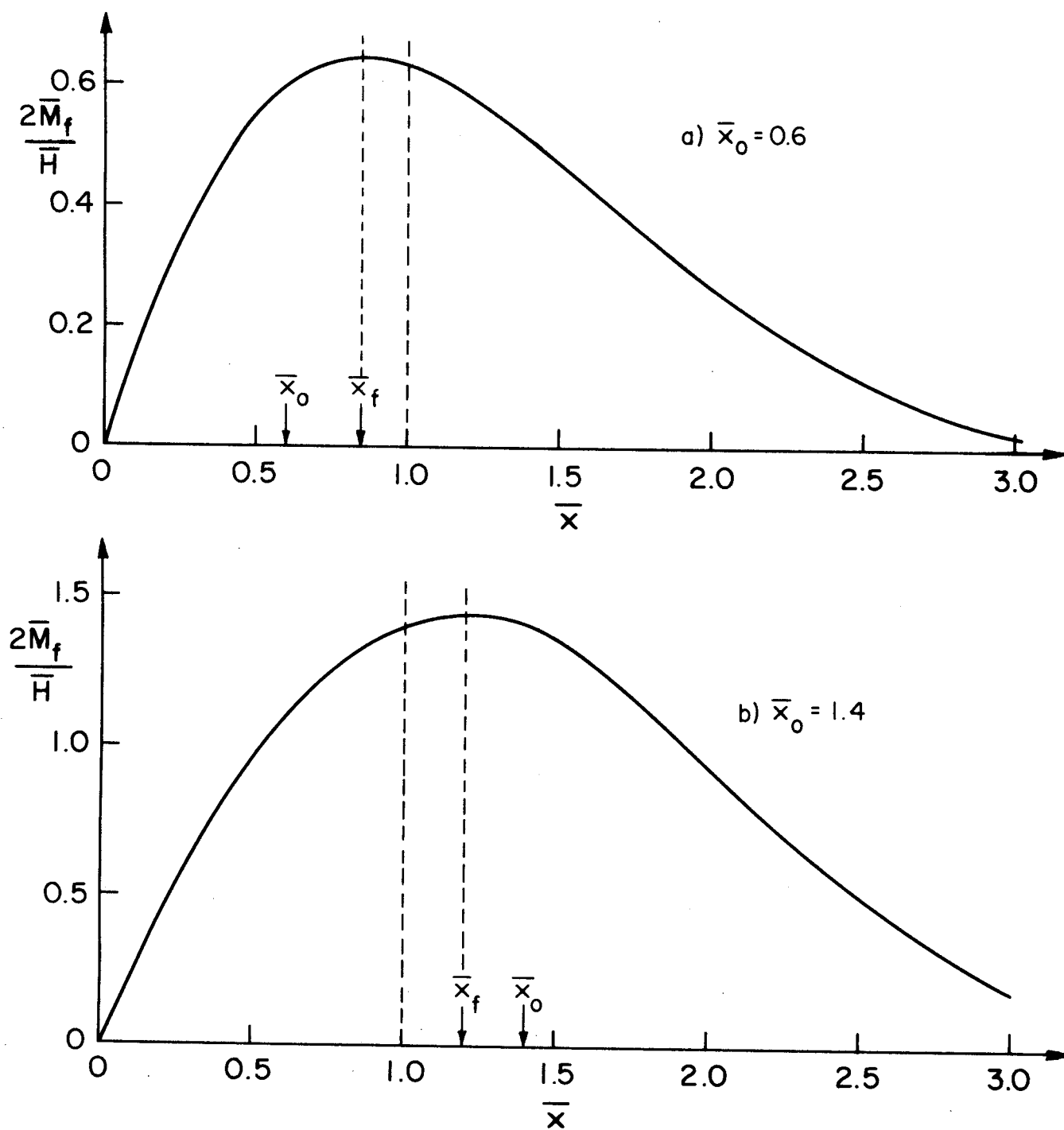


Figure 4. Examples of Bending Moment Distribution along Semi-Infinite Ice Sheet. a) $\bar{x}_0 = 0.6$; b) $\bar{x}_0 = 1.4$

and the corresponding expressions for \bar{M}_f are

$$\bar{M}_f = \frac{\bar{\sigma}_b}{2\bar{h}} = \frac{\bar{H}}{2} \sqrt{\frac{1 + \bar{x}_O^2}{2}} \exp\left(-\frac{\pi}{4} + \tan^{-1} \bar{x}_O\right) \text{ for } \bar{x}_O < 1 \quad (48a)$$

and

$$\bar{M}_f = \frac{\bar{\sigma}_b}{2\bar{h}} = \frac{\bar{H}}{2} \left(\frac{1 + \bar{x}_O}{2}\right)^2 \text{ for } \bar{x}_O > 1 \quad (48b)$$

Equations 48a and 48b are plotted as $2\bar{M}_f/\bar{H}$ versus \bar{x}_O on Figure 5. When $\bar{x}_O = 1$ then

$$\bar{x}_f = \bar{x}_O = 1$$

and

$$\bar{M}_f = \frac{\bar{H}}{2}$$

The results of the analysis for the case $\bar{x}_O > 1$ deserve further attention. Combination of equations 44 and 48b yields

$$\bar{F} = \bar{x}_f \bar{H} \quad (49a)$$

which can also be expressed as

$$\frac{F_f}{\gamma_w b H x_f} = 1 \quad (49b)$$

Furthermore by eliminating \bar{x}_O between equations 44 and 48b one obtains

$$\bar{F} = \sqrt{\frac{\bar{\sigma}_b}{\gamma_w} \frac{\bar{H}}{h}} \quad (50)$$

which, when the definition for L is introduced, can be written

$$\frac{F_f}{\gamma_w b h^2} = \sqrt{\frac{1}{3} \frac{\sigma_b}{\gamma_w} \frac{H}{h}} \quad (51a)$$

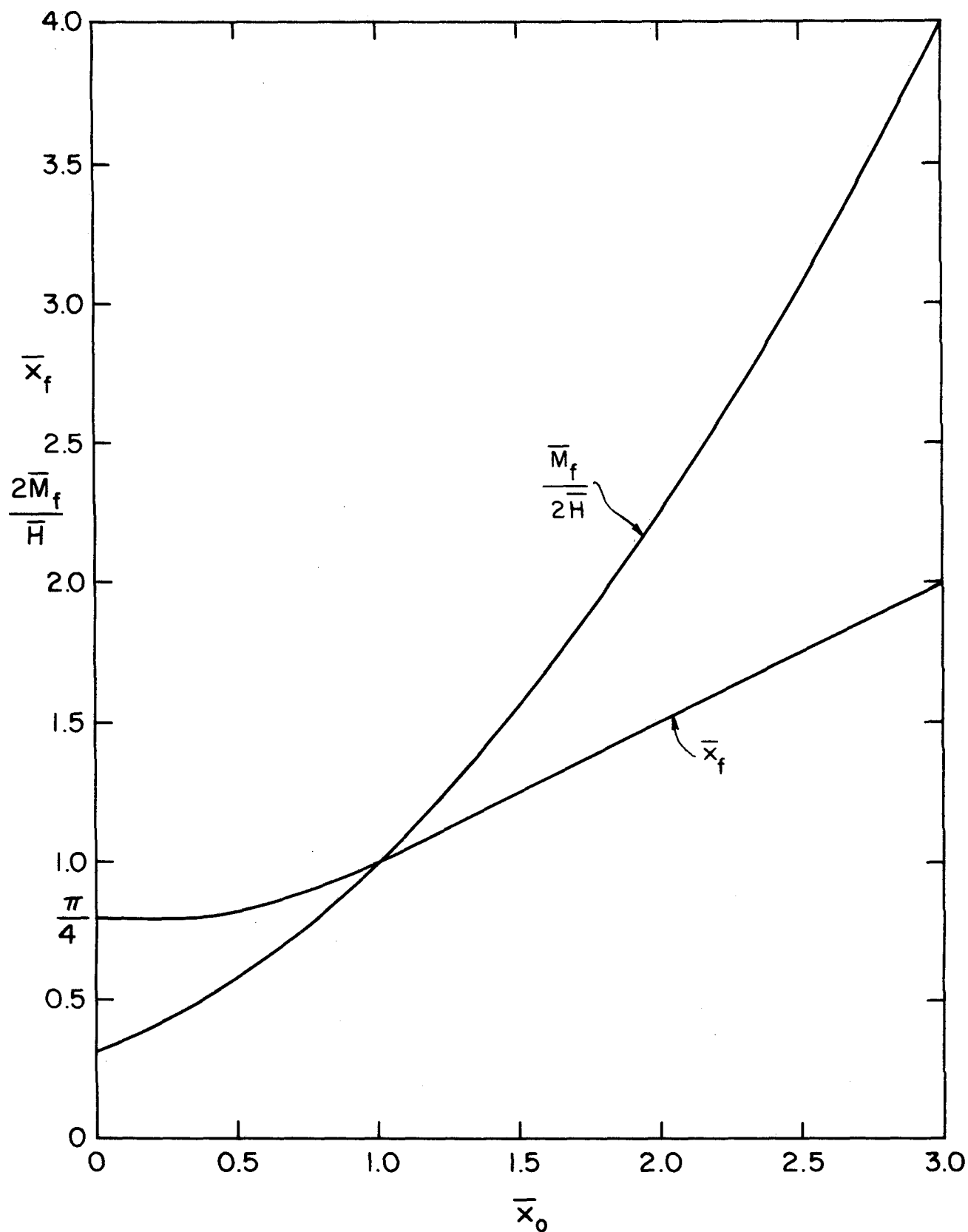


Figure 5. Maximum Bending Strength and Its Location \bar{x}_f as a Function of \bar{x}_0

while the expression for x_f can be reduced to

$$\frac{x_f}{h} = \sqrt{\frac{1}{3} \frac{\sigma_b}{\gamma_w} \frac{h}{H}} \quad (51b)$$

The above expressions show that, when $x_o/L > 1$, both F and x_f are independent of the elastic modulus E of the ice, and therefore of the ratio E/σ_b , and are proportional to the square root of $(\sigma_b/\gamma_w h)$. Only the displacement y_{o_f} will be function of E/σ_b , namely

$$\frac{y_o}{h} = \frac{8}{g} \left(\frac{h}{H}\right) \left(\frac{\sigma_b}{E}\right) \left(\frac{\sigma_b}{\gamma_w h}\right) + \frac{2\sqrt{2}}{3\sqrt[4]{3}} \sqrt{\frac{H}{h}} \sqrt[4]{\frac{\sigma_b}{E}} \sqrt[4]{\frac{\sigma_b}{\gamma_w h}} + \frac{1}{2} \frac{H}{h} \quad (51c)$$

The condition of application of equations 51a to 51c, namely, $x_o/L > 1$, can also be written, according to equation 48b, as

$$\frac{\sigma_b}{hH} \geq 1 \quad (52a)$$

or, when the definition for L is introduced, as

$$\frac{1}{\sqrt{3}} \left(\frac{\sigma_b}{E}\right)^{1/2} \left(\frac{\sigma_b}{\gamma_w h}\right)^{1/2} \left(\frac{h}{H}\right) \geq 1 \quad (52b)$$

that is

$$h \leq \frac{0.33}{\alpha} \frac{\sigma_b^2}{\gamma_w E} = h_{\min} \quad (53a)$$

or

$$\frac{E}{\sigma_b} \leq \frac{0.33}{\alpha} \left(\frac{\sigma_b}{\gamma_w h}\right) \quad (53b)$$

where $\alpha = H/h$ and can be expressed in terms of the ice specific gravity.

In summary, when the free end fully emerges from or submerges into the water, i.e., for $h > h_{\max}$ as defined by equation 40, the maximum forces F_f and P_f exerted by or on the ice can be determined as follows.

1. Calculate ϕ , α , L , $\bar{\sigma}_b = \sigma_b/E$, $\bar{h} = h/L$, $\bar{H} = H/L = \alpha\bar{h}$, and h_{\min} (equation 53a).

2. If $h > h_{\min}$, determine \bar{x}_o from equation 49a, \bar{x}_f from equation 47a, \bar{y}_{of} from equation 43b, and \bar{F}_f from equation 44. Convert to dimensional quantities x_f , y_{of} and F_f .

3. If $h < h_{\min}$, then F_f , x_f and y_{of} are obtained directly from equations 51a to 51c.

4. Calculate $P_f = \phi F_f$.

Example: An ice sheet of thickness $h = 15$ cm is being pushed up a beach inclined at $\theta = 30^\circ$. The coefficient of friction μ is 0.15, and the ice properties are

$$\sigma_b = 10^6 P_a$$

$$E = 2 \times 10^9 P_a$$

$$\rho_i/\rho_w = 0.92$$

$$1. \quad \alpha = \rho_i/\rho_w = 0.92; \quad \phi = \frac{\sin \theta + \mu \cos \theta}{\cos \theta - \mu \sin \theta} = 0.80$$

$$L = \sqrt[4]{\frac{Eh^3}{3\gamma_w}} = 3.89 \text{ m}$$

$$H = \alpha h = 13.80 \text{ cm}$$

$$h_{\max} = \frac{3.20}{\alpha^2} \frac{\sigma_b^2}{\gamma_w^3} = 0.193 \text{ m}$$

$$h_{\min} = 0.02 \text{ m}$$

2. Since $h < h_{\max}$, the edge of the ice sheet will emerge from the water before failure occurs, however, $h > h_{\min}$ and the equations for $\bar{x}_o < 1$ are to be applied.

Equation 48a yields $\bar{x}_O = 0.120$

Equation 47a yields $\bar{x}_f = 0.786$

Equation 43b gives $y_{O_f}/H = 1.14$

Equation 44 gives $\bar{F}_f = 1.99 \cdot 10^2$

The dimensional values are

$$F_f = 2950 \text{ N/m}$$

$$y_{O_f} = 15.7 \text{ cm}$$

$$x_f = 3.06 \text{ m}$$

C. Finite Ice Sheet ($P = M_O = 0$, $F \neq 0$)

1. Introduction. We have examined so far the case of a semi-infinite ice sheet moving against a sloping structure. However, in practical cases the ice sheet is seldom semi-infinite. Its actual size can vary from that of a river ice floe of relatively small dimensions striking a bridge pier or other structure, to that of a lake ice cover of very large dimension being pushed up a beach by wind shear. We will now examine the case of a finite ice sheet, to determine the length beyond which the ice sheet can be considered semi-infinite, and the equations derived in the previous chapter are applicable.

2. Governing Equation. The analysis of the deformation of a finite ice sheet of finite length l will be limited to the quasi-steady case, under the assumption that the lifting edge of the ice sheet never emerges from the water (i.e., $y_O \leq h_O$) and is subjected to only a lift force F . The horizontal force $P = 0$ and therefore $M_O = 0$. The corresponding governing equation in dimensionless form is

$$\frac{d^4 \bar{y}}{dx^4} + 4\bar{y} = 0 \quad (54)$$

The edge $\bar{x} = \bar{\ell}$ is a free end and is therefore subjected to no moment and no shear force. The boundary conditions at that location are

$$\frac{d^2 \bar{y}}{dx^2} = \frac{d^3 \bar{y}}{dx^3} = 0 \quad \text{at } \bar{x} = \bar{\ell} \quad (55)$$

At the lifting edge the boundary conditions are

$$\bar{M}_O = 0 \text{ or } \frac{d^2 \bar{y}}{dx^2} = 0 \quad \text{at } \bar{x} = 0 \quad (56)$$

and

$$\left. \frac{d^3 \bar{y}}{dx^3} \right|_{\bar{x}=0} = \int_0^{\bar{\ell}} \bar{y} \, d\bar{x} = 4\bar{F} \quad (57)$$

This last equation results from the combination of equations 23 and 23a with equation 55.

The general solution of equation 54 is of the form

$$\bar{y} = e^{-\bar{x}}(K_1 \cos \bar{x} + K_2 \sin \bar{x}) + e^{\bar{x}}(K_3 \cos \bar{x} + K_4 \sin \bar{x}) \quad (58)$$

The coefficients K_1 , K_2 , K_3 and K_4 are obtained in terms of \bar{F} from the above boundary conditions as

$$\begin{aligned} K_1 &= \frac{e^{2\bar{\ell}} - \sin(2\bar{\ell}) - 1}{\cosh(2\bar{\ell}) + \cos(2\bar{\ell}) - 2} \bar{F} \\ K_2 &= K_4 = \frac{1 - \cos(2\bar{\ell})}{\cosh(2\bar{\ell}) + \cos(2\bar{\ell}) - 2} \bar{F} \\ K_3 &= \frac{1 - \sin(2\bar{\ell}) - e^{-2\bar{\ell}}}{\cosh(2\bar{\ell}) + \cos(2\bar{\ell}) - 2} \bar{F} \end{aligned} \quad (59)$$

and the lifting edge displacement, \bar{y}'_O , is obtained from

$$\bar{y}'_0 = \bar{y} \Big|_{\bar{x}=0} = \frac{\sinh(2\bar{\ell}) - \sin(2\bar{\ell})}{\cosh(2\bar{\ell}) + \cos(2\bar{\ell}) - 2} 2\bar{F} \quad (60)$$

A semi-infinite ice sheet subjected to the same lifting force F as the finite ice sheet now considered has a displacement \bar{y}_0 given by

$$\bar{y}_0 = 2\bar{F}$$

therefore

$$\frac{\bar{y}'_0}{\bar{y}_0} = \frac{\sinh(2\bar{\ell}) - \sin(2\bar{\ell})}{\cosh(2\bar{\ell}) + \cos(2\bar{\ell}) - 2} \quad (61)$$

Also for a semi-infinite ice sheet it has been shown that $K_1 = 2\bar{F}$ while K_2, K_3 and K_4 are zero. Equations 59 do show that when ℓ increases, K_1 tends towards $2\bar{F}$ and K_2, K_3, K_4 tend to zero.

Table 1 presents the results of computations of $\bar{y}'_0/\bar{y}_0, \bar{K}_i/\bar{F}$ ($i = 1, 2, 3, 4$) for increasing value of ℓ . It can be seen that for $\ell = 3.0$, \bar{y}'_0 and K_1 are practically equal to \bar{y}_0 and $2\bar{F}$ respectively, and K_2, K_3, K_4 are negligibly small. Therefore, an ice flow of length

$$\ell = 3.0L = 3.0 \left(\frac{Eh}{3\gamma_w} \right)^{3/4} \quad (62)$$

can be considered to behave as a semi-infinite ice sheet.

When the length of the ice floe is less than $3.0L$, the force exerted on the structure can be calculated as follows:

1. The quantities $a_i = K_i/\bar{F}$ ($i = 1, 2, 3, 4$) are calculated according to equations (59).

2. The location, \bar{x}_f , of the maximum bending moment \bar{M}_f , is determined from $d\bar{M}/d\bar{x} = 0$ by solving numerically the equation

$$e^{-2\bar{x}_f} = \frac{(a_2 - a_3) \cos \bar{x}_f - (a_2 + a_3) \sin \bar{x}_f}{(a_1 - a_2) \sin \bar{x}_f - (a_1 + a_2) \cos \bar{x}_f} \quad (80)$$

3. The corresponding value of \bar{M}_f/\bar{F} is then given by

$$\frac{\bar{M}_f}{\bar{F}} = \frac{1}{4\bar{F}} \frac{d^2 \bar{y}}{d\bar{x}^2} \Big|_{\bar{x} = \bar{x}_f}$$

$$= a_2 \cos \bar{x}_f \sinh \bar{x}_f + \frac{1}{2} (a_1 e^{-\bar{x}_f} - a_3 e^{\bar{x}_f}) \sin \bar{x}_f \quad (61)$$

4. The maximum bending moment at failure is related to the bending strength of the ice by

$$\bar{\alpha}_b = 2 \bar{M}_f \bar{h}$$

which yields the expression for the failure force

$$\bar{F}_f = \frac{\bar{\alpha}_b}{2\bar{h}(\bar{M}_f/\bar{F})} \quad (62)$$

5. The corresponding displacement of the lifting edge is then obtained as

$$\bar{y}'_{O_f} = (a_1 + a_3) \bar{F}_f \quad (63)$$

D. Discussion

Since the influence of the horizontal force P and moment M_O on the vertical failure force F_f appears to be minor, the following discussion is limited to the case $P = M_O = 0$, and is expected to be valid when P and M_O are non zero.

In the experimental studies and modelling of forces exerted by monolithic ice sheets on inclined structures, in particular in ice breakers model tests, it has been recognized that the two parameters E/σ_b and $\sigma_b/\gamma_w h$ were to be the same at model and prototype scales. From the previous analysis, the force F_f , length x_f and displacement y_{O_f} , for the case of two-dimensional structure can, in their dimensionless forms $F_f/\gamma_w b h^2$, x_f/h and y_{O_f}/h , indeed be expressed as functions of these two parameters only, namely

$$1. \text{ For } E/\sigma_b \geq \frac{3.20}{\alpha} \frac{\sigma_b}{\gamma_w h}$$

Table 1. Comparison Between Finite and Semi-Infinite Ice Sheets

\bar{x}	y_o/\bar{y}_o	K_1/\bar{F}	$K_2, K_4/\bar{F}$	K_3/\bar{F}
0.5	4.002	1.052	-5.513	-2.511
1.0	2.019	4.071	-1.052	-0.033
1.5	1.395	2.677	-0.281	0.114
2.0	1.138	2.205	-0.067	0.071
2.5	1.037	2.047	-9.9 E-4	0.027
3.0	1.007	2.007	-2.0 E-4	6.4 E-3
3.5	1.001	2.002	-4.5 E-4	6.3 E-4
4.0	1.001	2.002	-7.7 E-4	6.9 E-6
5.0	1.00	2.000	-1.7 E-4	1.4 E-4

$$\frac{F_f}{\gamma_w b h^2} = 0.68 \left(\frac{E}{\sigma_b}\right)^{-1/4} \left(\frac{\sigma_b}{\gamma_w h}\right)^{3/4} \quad (64a)$$

$$\frac{x_f}{h} = 0.60 \left(\frac{E}{\sigma_b}\right)^{1/4} \left(\frac{\sigma_b}{\gamma_w h}\right)^{1/4} \quad (65a)$$

$$\frac{y_{of}}{h} = 1.79 \left(\frac{E}{\sigma_b}\right)^{-1/2} \left(\frac{\sigma_b}{\gamma_w h}\right)^{1/2} \quad (66a)$$

with also the relationship

$$\frac{F}{\gamma_w b h x_f} = \frac{2}{\pi} \frac{y_{of}}{h} \quad (67)$$

$$2. \quad \text{For } \frac{0.33}{\alpha} \frac{\sigma_b}{\gamma_w h} \leq E/\sigma_b \leq \frac{3.20}{\alpha} \frac{\sigma_b}{\gamma_w h}$$

$$\frac{F_f}{\gamma_w b h^2} = \frac{\alpha}{2} \left(\frac{L}{h} + \frac{x_o}{h}\right) \quad (64b)$$

$$\frac{x_f}{h} = \frac{x_o}{h} + \frac{L}{h} \left[\frac{\pi}{4} - \tan^{-1} \left(\frac{x_o}{h} \frac{h}{L} \right) \right] \quad (65b)$$

$$\frac{y_{of}}{h} = \frac{\alpha}{6} \left[\left(1 + \frac{x_o}{L}\right)^4 + 2 \left(1 + \frac{x_o}{L}\right) + 3 \right] \quad (66b)$$

where $\frac{x_o}{L} = \frac{x_o}{h} \cdot \frac{h}{L}$ is solution of

$$\frac{\sigma_b}{E} = \alpha \left(\frac{h}{L}\right)^2 \sqrt{\frac{1 + (x_o/L)^2}{2}} \exp \left[-\frac{\pi}{4} + \tan^{-1} \left(\frac{x_o}{L} \right) \right] \quad (68)$$

and

$$\frac{L}{h} = \sqrt{\frac{1}{3} \left(\frac{E}{\sigma_b}\right) \left(\frac{\sigma_b}{\gamma_w h}\right)} \quad (69)$$

and $\alpha = H/h$

No explicit expression similar to equation (67) could be obtained in the present range of E/σ_b .

$$3. \text{ For } E/\sigma_b \leq \frac{0.33}{\alpha^2} \frac{\sigma_b}{\gamma_w h}$$

$$\frac{F_f}{\gamma_w b h^2} = \frac{\sqrt{\alpha}}{3} \left(\frac{\sigma_b}{\gamma_w h} \right)^{1/2} \quad (64c)$$

$$\frac{x_f}{h} = \sqrt{\frac{1}{3\alpha}} \left(\frac{\sigma_b}{\gamma_w h} \right)^{1/2} \quad (65c)$$

$$\frac{y_o}{h} = \frac{8}{9\alpha} \left(\frac{\sigma_b}{B} \right) \left(\frac{\sigma_b}{\gamma_w h} \right) + 0.358 \sqrt{\alpha} \left(\frac{\sigma_b}{E} \right)^{1/4} \left(\frac{\sigma_b}{\gamma_w h} \right)^{1/4} + 0.50 \alpha \quad (66c)$$

while

$$\frac{x_o}{h} = 2 \frac{x_f}{h} - \frac{L}{h} \quad (70)$$

and also

$$\frac{F_f}{\gamma_w b h x_f} = \alpha \quad (71)$$

For future use, the quantities $F^* = \frac{F_f}{\gamma_w b x_f H}$ and $\frac{x_o}{L}$ were plotted versus $y^* = y_o/H$ on figure 6.

An important result is that when the ice stiffness $S = E/\sigma_b$ is below the critical value $S_c = \frac{0.33}{\alpha^2} \frac{\sigma_b}{\gamma_w h}$, the failure force F_f and the break length x_f become independent of S , only the displacement y_o remains dependent upon the stiffness E/σ_b . The result has important implications. Consider in particular the dynamics of ice breakers and the problem of

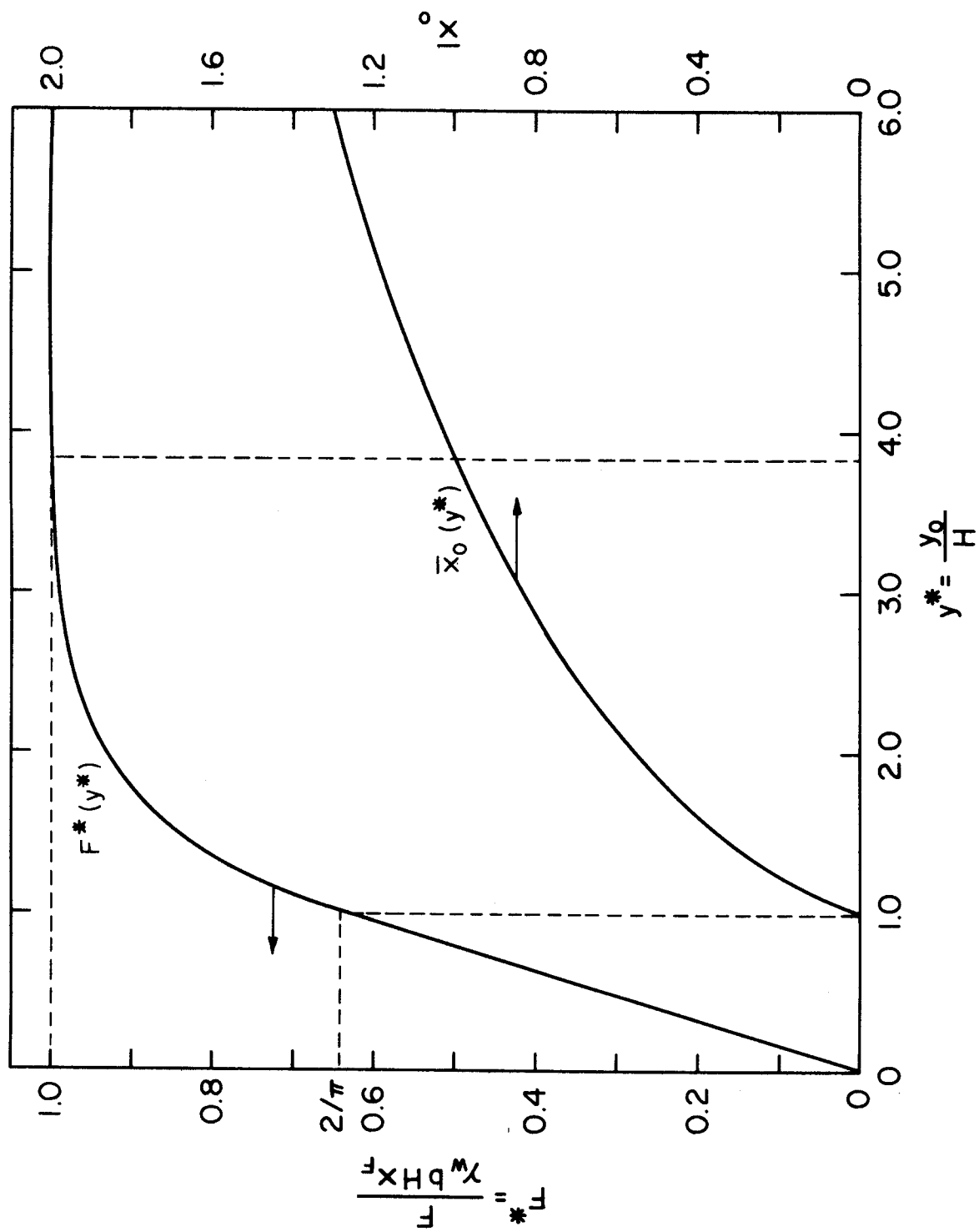


Figure 6. Plot of F^* and \bar{x}_0 versus y_0/H

ice breakers model tests. There exists a long running controversy on the proper reduction to model scale of the mechanical properties of ice. The correct scaling of the ice bending strength σ_b is usually achieved by using doped ice (either saline or urea ice), however the elastic modulus at scales less than 1/20 becomes too small and the ratio E/σ_b in the model is much lower than that in the prototype. But if the prototype value of $S = E/\sigma_b$ is less than its critical value S_c , then the model-ice stiffness could be lower than the prototype value without affecting the force F_f , as long as the model ice behaves elastically since all the above results were obtained assuming that elastic theory applied. For example, if for sea-ice the values $\sigma_b = 10^3 \text{ kPa}$, $\rho_i/\rho_w = 0.91$, and $\gamma_w = 9810 \text{ N/m}^3$ are adopted, since ice breakers exert a downward force on the ice the corresponding value of α is $\alpha = 1 - \rho_i/\rho_w = 0.09$. For an ice thickness h of 2 m, F_f is independent of E/σ_b if E/σ_b is less than 2000; when $E/\sigma_b = 5000$, the force F_f will become independent of E/σ_b for ice thicknesses less than 0.80 m.

The dimensionless force $F^0 = F_f/\gamma_w b h^2$ has been plotted versus $\sigma^0 = \sigma_b/\gamma_w h$, with E/σ_b as a parameter, on Figure 7, and versus E/σ_b , with σ^0 as a parameter, on Figure 8. In these figures the value $\alpha = 0.09$ was selected.

IV. SOLUTION OF THE UNSTEADY EQUATION ($M_0 = P = 1$, $F \neq 0$)

Since according to the analysis of the steady form of equation 15, the effect of M_0 and P on the horizontal force F exerted by an ice sheet on an inclined plane is relatively minor, only the case $M_0 = P = 0$ will be treated here. Furthermore only the case when failure occurs prior to the complete emergence or submergence of the leading edge will be considered. The governing equation is then

$$\frac{\partial^4 \bar{y}}{\partial x^4} + 4(\bar{y} + \frac{\partial^2 \bar{y}}{\partial t^2}) = 0 \quad (72)$$

with the initial conditions

$$\bar{y}(\bar{x}, 0) = 0 \text{ all } x \quad (73a)$$

$$\left. \frac{\partial \bar{y}}{\partial t} \right|_{t=0} = 0 \text{ all } x \quad (73b)$$

and the boundary conditions

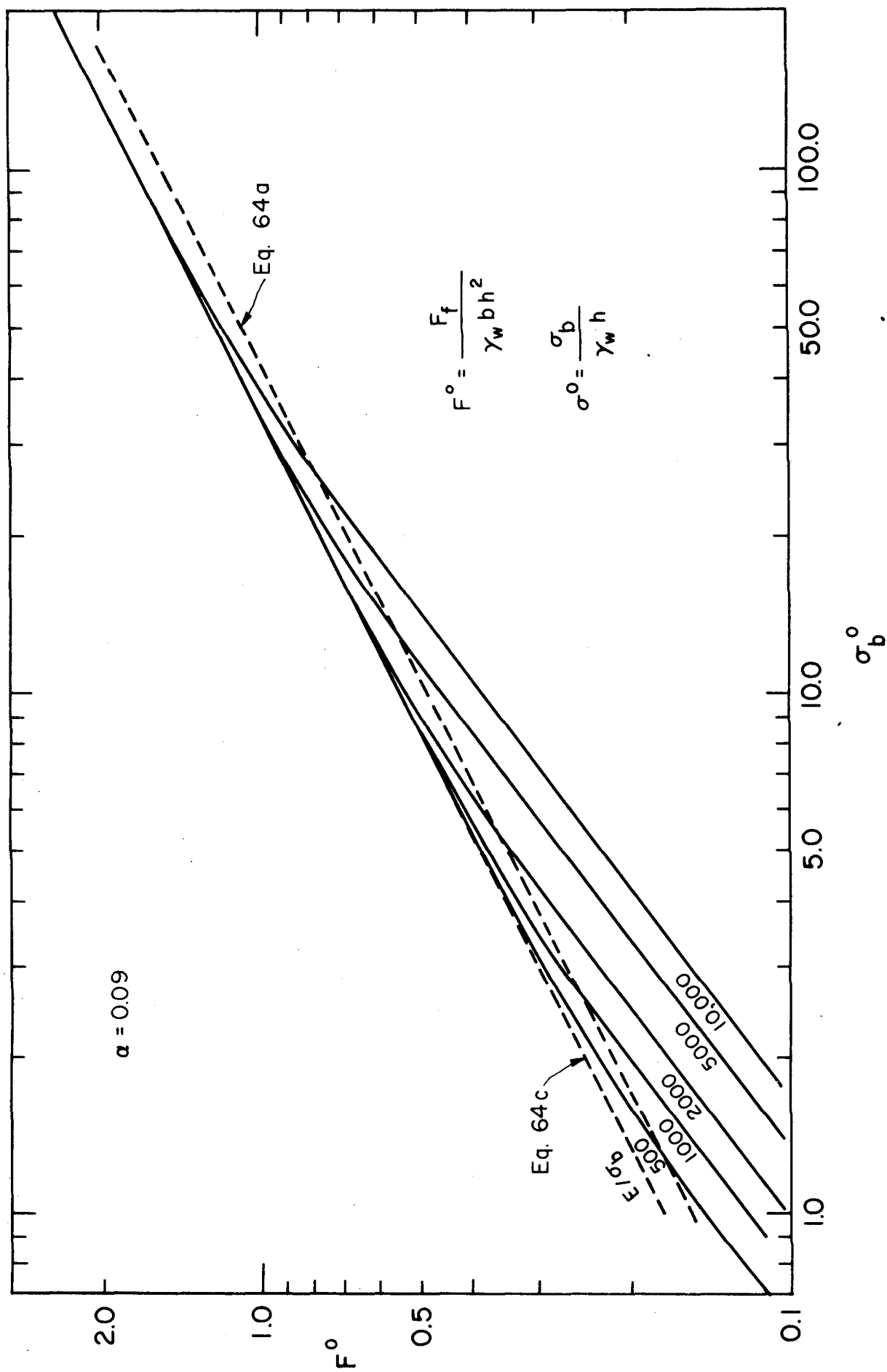


Figure 7. Plot of F^0 versus σ_b^0 with E/σ_b as Parameter

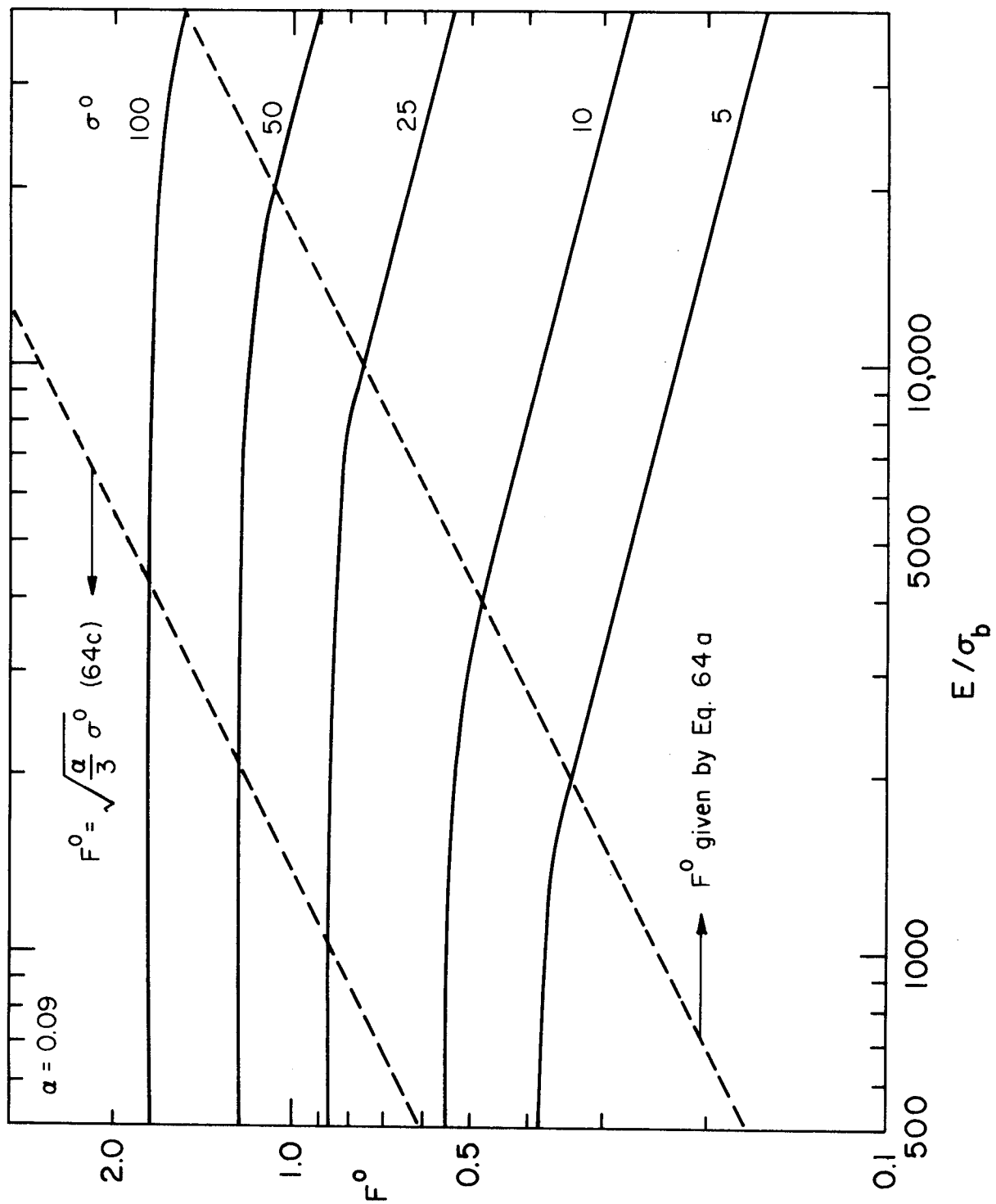


Figure 8. Plot of F^0 versus E/σ_b with σ^0 as Parameter

$$\bar{y} = \frac{\partial n^-}{\partial \bar{x}} = 0 \text{ as } \bar{x} \rightarrow \infty \quad (74)$$

$$\left. \frac{\partial^2 \bar{y}}{\partial \bar{x}^2} \right|_{\bar{x}=0} = 0 \quad (75a)$$

$$\left. \frac{\partial \bar{y}}{\partial \bar{t}} \right|_{\bar{x}=0} = \frac{d\bar{y}_0(\bar{t})}{d\bar{t}} = \bar{u}_0 (1 - e^{-k\bar{t}}) \quad (75b)$$

where k is some arbitrary large coefficient.

The form of the boundary condition given by equation 75b was chosen so that it can be compatible with equation 73b, and that the vertical velocity of the leading edge reaches a practically constant value after a short time.

The Laplace transform with respect to time of equation 72 is

$$\frac{\partial^4 y_s}{\partial \bar{x}_4} + 4(1 + s^2) y_s = 0 \quad (76)$$

with

$$y_s(\bar{x}, s) = L \left[\bar{y}(\bar{x}, \bar{t}) \right] = \int_0^\infty e^{-s\bar{t}} \bar{y}(\bar{x}, \bar{t}) d\bar{t}$$

The boundary conditions become

$$y_s = \frac{\partial n^-}{\partial \bar{x}} = 0 \text{ as } \bar{x} \rightarrow \infty \quad (77)$$

$$\left. \frac{\partial^2 y_s}{\partial \bar{x}^2} \right|_{\bar{x}=0} = 0 \quad (78a)$$

$$y_s(0, s) = y_{s0} = \bar{u}_0 \frac{k}{s^2(s+k)} \quad (78b)$$

Introducing the change of variable $x_s = \bar{x} \sqrt{1+s^2}$ into equation 75 one obtains

$$\frac{d^4 y_s}{dx_s^4} + 4y_s = 0 \quad (79)$$

which, for the given boundary conditions, has the solution

$$y_s = \frac{\bar{u}_0 k}{s^2(s+k)} e^{-x_s} \cos x_s \quad (80)$$

According to equation 23 with $\bar{x}_0 = 0$, the force \bar{F} is given by

$$\bar{F}(\bar{t}) = \int_0^\infty \left(\bar{y} + \frac{\partial^2 \bar{y}}{\partial \bar{t}^2} \right) d\bar{x} = \frac{1}{4} \frac{\partial^3 \bar{y}}{\partial \bar{x}^3} \Big|_{\bar{x}=0}$$

the Laplace transform F_s of $\bar{F}(\bar{t})$ is then

$$F_s = \frac{\bar{u}_0 k(1+s^2)^{3/4}}{2s^2(s+k)} = \frac{\bar{u}_0 k (1+s^2)}{2s^2(s+k) \sqrt{1+s^2}} \quad (81)$$

or

$$F_s = \frac{\bar{u}_0}{2} \frac{1}{(1+s^2)^{1/4}} \left(\frac{1}{s} - \frac{1}{ks} + \frac{1+k^2}{k} \cdot \frac{1}{s+k} \right) \quad (82)$$

The inverse Laplace transforms of the various functions appearing in equation 82 are

$$L^{-1} \left[\frac{1}{(1+s^2)^{1/4}} \right] = \frac{\sqrt{\pi}}{\Gamma(1/4)} \left(\frac{\bar{t}}{2} \right)^{-1/4} J_{-1/4}(\bar{t}) = \frac{\sqrt{\pi}}{\Gamma(1/4)} G(\bar{t})$$

$$L^{-1} \left[\frac{1}{s} \right] = \bar{t}$$

$$L^{-1} \left[\frac{1}{s} \right] = 1$$

$$L^{-1} \left[\frac{1}{s+k} \right] = e^{-k\bar{t}}$$

where $J_\lambda(t)$ is the Bessel function of the first kind of order λ . Therefore the force $\bar{F}(\bar{t})$, obtained as the inverse Laplace transform of F_s , is given by

$$\bar{F}(\bar{t}) = \frac{\bar{u}_0 \sqrt{\pi}}{2\Gamma(1/4)} \int_0^{\bar{t}} \left\{ \int_0^\tau G(\lambda) d\lambda - \frac{G(\tau)}{k} + \frac{1+k^2}{k} G(\tau) e^{-k(\bar{t}-\tau)} \right\} d\tau \quad (83)$$

Bessel functions of the first kind $J_\lambda(x)$ can be expressed as infinite series in x , namely

$$J_{\lambda}(x) = \sum_{n=0}^{\infty} \frac{(-1)^n}{n! \Gamma(n+\lambda+1)} \left(\frac{x}{2}\right)^{2n+\lambda} \quad (84)$$

therefore the function $G(\bar{t})$ can be expressed as

$$G(\bar{t}) = \left(\frac{\bar{t}}{2}\right)^{-1/4} J_{-1/4}(\bar{t}) = \sum_{n=0}^{\infty} \frac{(-1)^n}{n! \Gamma(n+\frac{3}{4})} \left(\frac{\bar{t}}{2}\right)^{2n-\frac{1}{2}} \quad (85)$$

When this expression for $G(\bar{t})$ is introduced into equation 83, the various integrations may be performed to yield

$$\begin{aligned} \bar{F}(\bar{t}) = \frac{2\bar{u}_o \sqrt{\pi}}{\Gamma(1/4)} \sum_{n=0}^{\infty} \frac{(-1)^n}{n! \Gamma(n+\frac{3}{4})} \left(\frac{\bar{t}}{2}\right)^{2n+\frac{1}{2}} \left\{ \frac{4\bar{t}^2}{(4n+1)(4n+3)} - \frac{1}{k(4n+1)} \right. \\ \left. + \frac{1+k^2}{k} \frac{e^{-k\bar{t}}}{\sum_{p=0}^{\infty} \frac{(k\bar{t})^p}{p!(4n+2p+1)}} \right\} \quad (86) \end{aligned}$$

The moment distribution in the ice sheet is given by

$$\bar{M}(\bar{x}, \bar{t}) = \frac{1}{4} \frac{\partial^2 \bar{y}}{\partial \bar{x}^2}$$

the Laplace transform of which is

$$M_s(\bar{x}, \bar{t}) = \frac{1}{4} \frac{\partial^2 \bar{y}_s}{\partial \bar{x}^2} = \frac{\bar{u}_o k \sqrt{1+s^2}}{2s^2(s+k)} e^{-x_s} \sin x_s \quad (87)$$

the maximum of M_s is then given by

$$M_{sf} = 0.161 \frac{\bar{u}_o k \sqrt{1+s^2}}{s^2(s+k)} = 0.161 \bar{u}_o \frac{1}{\sqrt{1+s^2}} \left\{ \frac{1}{s^2} - \frac{1}{ks} + \frac{1+k^2}{k} \frac{1}{s+k} \right\} \quad (88)$$

The maximum bending moment \bar{M}_f is obtained as the Laplace transform of M_{sf} , i.e.,

$$\bar{M}_f = 0.161 \bar{u}_o \int_0^{\bar{t}} \left\{ \int_0^{\tau} J_o(\lambda) d\lambda - \frac{J_o(\tau)}{k} + \frac{1+k^2}{k} J_o(\tau) e^{-k(\bar{t}-\tau)} \right\} d\tau \quad (89)$$

When J_o is replaced by its infinite series expansion

$$J_o(x) = \sum_{n=0}^{\infty} \frac{(-1)^n}{(n!)^2} \left(\frac{x}{2}\right)^{2n} \quad (90)$$

equation 89 becomes

$$\bar{M}_f = 0.161 \bar{u}_o \sum_{n=0}^{\infty} \frac{(-1)^n}{(n!)^2} \left\{ \frac{2}{2n+1} \left(\frac{\bar{t}}{2}\right)^{2n+1} \left(\frac{\bar{t}^2}{4} - \frac{1}{k}\right) + \frac{1+k^2}{k^{2n+2}} \frac{(2n)!}{2^{2n}} \left[\sum_{p=0}^{2n} \frac{(-1)^p (k\bar{t})^{2n-p}}{(2n-p)!} - e^{-k\bar{t}} \right] \right\} \quad (90)$$

which can also be written as

$$\bar{M}_f = 0.161 \bar{u}_o \sum_{n=0}^{\infty} \frac{(-1)^n}{(n!)^2} \left\{ \frac{2}{2n+1} \left(\frac{\bar{t}}{2}\right)^{2n+1} \left(\frac{\bar{t}^2}{4} - \frac{1}{k}\right) - \frac{1+k^2}{k^2} \frac{(2n)!}{2^{2n}} \sum_{p=2n+1}^{\infty} (-1)^p \frac{k^{p-2n-p} \bar{t}^p}{p!} \right\} \quad (91)$$

when the expansion of $e^{-k\bar{t}}$ is used, namely

$$e^{-k\bar{t}} = \sum_{p=0}^{\infty} (-1)^p \frac{(k\bar{t})^p}{p!}$$

Failure of the ice sheet occurs when the maximum bending moment satisfies the relationship

$$\bar{M}_f = \frac{\bar{\sigma}_b}{2\bar{h}} \quad (92)$$

where $\bar{\sigma}_b$ is the bending strength of the ice.

Thus, the time of failure \bar{t}_f can be determined from equating the right-hand sides of equations 91 and 92. Once \bar{t}_f is determined the force exerted by the ice on the structure is given by equation 86 for $\bar{t} = \bar{t}_f$.

VI. EXPERIMENTAL VERIFICATION AND APPLICATION

A. Preliminary Considerations

The foregoing analysis enable to predict the maximum force, F_f , exerted by an ice sheet on an inclined structure, the vertical displacement y_{of} at failure of the edge of the ice sheet and the length x_f of the broken floe once the mechanical properties, σ_b and E , of the ice are known. Conversely, the strength index and elastic index of the ice can be determined from lift-up or push-down experiments in which at least two of the three quantities F_f , y_{of} and x_f are measured. In fact, if these three parameters are measured simultaneously, then each pair $F_f - y_{of}$, $y_{of} - x_f$, and $x_f - F_f$ can be used to calculate E and σ_b . The three sets of E and σ_b determined should be nearly identical, within the limits of experimental accuracy, if the assumptions underlying the analysis are satisfied, in particular if the ice behaves like an elastic material.

The experimental program undertaken at the Iowa Institute of Hydraulic Research to verify and apply the previous analyses was divided into three phases.

Phase 1.

In a series of initial experiments the bending strength and elastic modulus of freshwater ice were determined and compared with values available in the literature. Freshwater ice under sufficiently high rate of strain has been shown to behave elastically and its mechanical properties are well documented.

Phase 2.

In a second experimental phase, an instrumented inclined plane of variable angle of inclination was built. Forces exerted by a freshwater ice sheet pushed at constant speed against this structure were measured and compared with the theoretical predictions where the values of σ_b and E determined in the initial experiments were used.

Phase 3.

The results of experimental phases 1 and 2 were judged satisfactory. The third phase was concerned with the determination of the strength index and modulus index of carbamide (urea)-doped ice which has been proposed by Timco (1979) as a substitute for saline ice as model ice in model studies of ice forces on structures. This third experimental phase is still underway and only preliminary results are presented here.

All the experiments conducted to date have been performed in the 19 ft x 3 ft x 2 ft (5.80 m x 0.91 m x 0.61 m) ice force tank of the Low Temperature Flow Facility (LTFF) of IIHR. The ice sheets grown in the tank were made free from the tank walls by placing a heating tape in a narrow sheet-metal trough mounted at water level along the perimeter of the tank. The experimental apparatus and procedures specific to each series of tests are described in the following relevant sections.

Since phases 1 and 3 above are concerned with the experimental determination of the mechanical properties, σ_b and E , of ice, the various methods of data analysis used to that purpose and based on the analytical approach developed in the previous chapter are first presented in the following section.

B. Methods of Calculations of σ_b and E

As mentioned in Section A above, the mechanical properties of an ice sheet, namely the bending strength index σ_b and the elastic modulus index E , can theoretically be calculated from experiments in which the free floating ice sheet is subjected to a pure lift or push at one end, and when two of the three parameters, y_{of} , the displacement at failure of the lifted or pushed end, F_f , the force at failure exerted on the ice, and x_f , the breaking length of the ice sheet are measured.

It is assumed that the following data are known

- l : initial length of ice sheet
- b : width of ice sheet
- h : thickness of ice sheet
- ρ_i : ice density
- ρ_w : water density

therefore the quantity H can be calculated

$$H = \rho_i / \rho_w h \text{ (lifting case)}$$

$$H = (1 - \rho_i / \rho_w) h \text{ (pushing case)}$$

In the following only quasi-steady conditions are considered, and the length ℓ is assumed to be sufficient for the ice sheet to be considered as semi infinite.

The results of the preceding analyses with $M_0 = P = 0$ are collected below for future reference

$$L = \sqrt{\frac{Eh^3}{3\gamma_w}} = h \sqrt{\frac{E}{3\gamma_w h}} \quad (13)$$

$$y_{of}/H \ll 1 \quad F_f = 0.68 \left(\frac{\gamma_w h}{E}\right)^{1/4} \sigma_b bh \quad (38a)$$

$$y_{of} = 1.79 \left(\frac{\gamma_w h}{E}\right)^{1/2} \frac{\sigma_b}{\gamma_w} \quad (38b)$$

$$x_f = 0.60 h \left(\frac{E}{\gamma_w h}\right)^{1/4} = \frac{\pi}{4} L \quad (38c)$$

$$\text{also} \quad F_f = \frac{2}{\pi} \gamma_w b x_f y_{of} = \frac{\gamma_w b L}{2} y_{of} \quad (93)$$

$$y_{of}/H \gg 1$$

$$\frac{y_{of}}{H} = \frac{1}{\gamma} \left[\left(1 + \frac{x}{L}\right)^4 + 2\left(1 + \frac{x}{L}\right) + 3 \right] \quad (43b)$$

$$\frac{F_f}{\gamma_w b L H} = \frac{1}{2} \left(1 + \frac{x_O}{L}\right) \quad (44)$$

$$x_O/L < 1$$

$$\frac{x_f}{L} = \frac{x_O}{L} + \frac{\pi}{4} - \tan^{-1} \left(\frac{x_O}{L}\right) \quad (47a)$$

$$\frac{\sigma_b}{E} = \frac{H}{L} \frac{h}{L} \sqrt{\frac{1 + (x_O/L)^2}{2}} \exp \left[-\frac{\pi}{4} + \tan^{-1} \left(\frac{x_O}{L}\right) \right] \quad (48a)$$

$$x_o/L > 1$$

$$\frac{x_f}{L} = \frac{1 + x_o/L}{2} \quad (47b)$$

$$\frac{\sigma_b}{E} = \frac{H}{L} \frac{h}{L} \left(\frac{1 + x_o/L}{2} \right)^2 \quad (48b)$$

For the latter case ($y_{of}/H > 1$, $x_o/L > 1$), it has been shown that

$$\frac{F_f}{\gamma_w b H x_f} = 1 \quad (49b)$$

and combination of equations 13, 68b and 69b results in

$$\sigma_b = 3\gamma_w \frac{H x_f^2}{h^2} = 3\alpha\gamma_w \frac{x_f^2}{h} \quad (94)$$

1. The y-F method:

The deflection y_{of} and force F_f are measured. The unknowns are x_f , L , E and σ_b , and x_o when $y_{of}/H > 1$.

a) $y_{of}/H < 1$: The characteristic length L is obtained from equation 93

$$L = \frac{2F_f}{\gamma_w b y_{of}} \quad (95)$$

then E is obtained from equation 13 as

$$E = \frac{3\gamma_w L^4}{h^3} \quad (96)$$

and σ_b and x_f are given by

$$\sigma_b = \frac{F_f^2}{\gamma_w b h^2 y_{of}} = \frac{F_f L}{2h^2} \quad (97)$$

$$x_f = \frac{\pi}{4} L = \frac{\pi F_f}{2\gamma_w b y_{of}} \quad (38c)$$

b) $y_{of}/H > 1$: the ratio x_o/L is calculated from equation 43b. Then L can be obtained from equation 44, E from equation 13, x_f from equation 47a or 49b, and σ_b from equation 69b or 84, depending whether x_o/L is smaller or greater than 1, respectively.

2. The x-y method:

The deflection y_{of} and length x_f of the broken floes are measured. The unknowns are F_f, L, E and σ_b , and x_o if $y_{of}/H > 1$.

a) $y_{of}/H < 1$: The length L and elastic modulus E are calculated from 38c, σ_b from equation 38b, and F_f from equation 38a.

b) $y_{of}/H > 1$: x_o/L is calculated from equation 43b, L can then be determined from equation 47a if $x_o/L < 1$, or equation 47b if $x_o/L > 1$. F_f is calculated from equation 44, and E from equation 13. Finally σ_b is calculated from equation 48a if $x_o/L < 1$, or from equation 84 if $x_o/L > 1$.

3. The x-F method:

The floe length x_f and force F_f are measured. The unknowns are y_{of}, L, E , and σ_b , and x_o when applicable.

The quantity $F^* = F_f / \gamma_w b H x_f$ is calculated, three cases are possible

a. $F^* < 2/\pi$: then y_{of}/H must be less than 1. L and E are determined from equation 38c, σ_b from equation 38a and y_{of} from equation 38b.

b. $2/\pi < F^* < 1$: y_{of}/H must be greater than 1, but x_o/L less than 1. Combining equations 44 and 47a one obtains the following equation for x_o/L

$$\frac{x_o}{L} = \tan \left[\frac{x_o}{L} \left(1 - \frac{1}{2F^*} \right) + \pi/4 - \frac{1}{2F^*} \right] \quad (98)$$

which yields a unique solution for $0 < x_o/L < 1$.

Then L can be determined from equation 44, y_{of} from equation 43b, E from equation 13, and σ_b from equation 48a.

c. $F^* = 1$: Then x_o/L must be greater than or equal to 1, and y_{of}/H equal to or greater than 23/6. The only quantity which can be determined is σ_b from equation 94. The elastic modulus E is undetermined since both F_f and x_f are independent of E .

C. Initial Experiments

1. Experimental Apparatus and Procedures:

The initial series of tests (Phase 1, above) consisted in lifting one end of a freshwater ice sheet at a constant speed U_o . Each ice sheet tested was grown in the LITF force tank at a room temperature of -10°C , approximately. Since it was not the purpose of these tests to model a particular ice, the ice sheet was not initially seeded but left to grow naturally.

The instrumented lifting device consisted of a horizontal angle iron spanning the width of the tank and suspended to a moment-insensitive dynamometer by two vertical bars. The dynamometer was attached to a vertical, square-threaded rod passing through a threaded bevel gear forming one part of a right angle speed reducer. The bevel gear was entrained by a smaller gear mounted on the shaft of a variable speed, D.C. motor. The motor speed was measured by a light-interruptor sensor set over the perforated edge of a disk mounted on the motor shaft. A specially designed and built counter counted the number of holes sensed by the light-interruptor and converted it into a voltage proportional to the vertical displacement of the lifting apparatus. The 10-volt full scale of the counter corresponded to 5 mm of vertical displacement. The counter reset itself to zero when reaching its full scale, so that the vertical displacement was obtained as multiple of 5-mm increments and portions. The vertical force F exerted on the lifting devices was measured by a combination of a load cell (Statham #UL-4) and a transducer (Statham #UC-2) mounted on the dynamometer. Both the vertical displacement y_o and the force F were continuously recorded on a Beckman multiple channels recorder. A sketch of the experimental apparatus is shown in Figure 9.

Failure of the ice sheet was indicated by a sudden drop in the force record. Maximum force, F_f , and corresponding displacement,

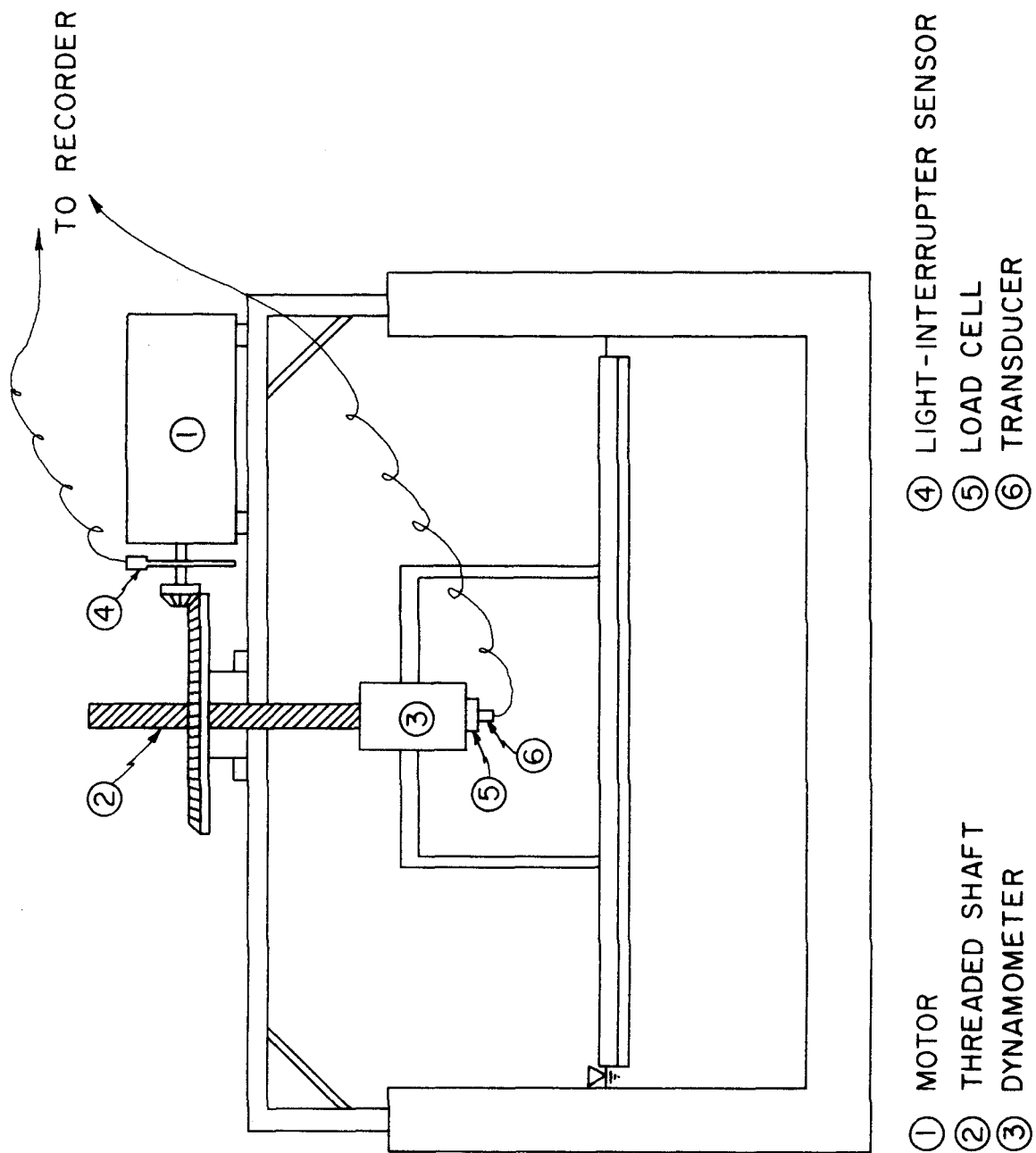


Figure 9. Sketch of Experimental Lift-Push Apparatus

y_{of} , were measured from the records. The length of the broken floe, x_f , was also measured. From these data, the characteristics σ_b and E of the ice were evaluated by the three methods discussed in the preceding section.

2. Experimental Results

Six freshwater ice sheets of various thicknesses were tested. Since all the ice sheets were grown in the same manner, their mechanical properties ought to be the same within the limits of experimental accuracy and validity of the analysis.

The experimental data and results of the analyses are presented in Table 2. Since all the sheets were relatively thin and stiff, failure always occurred after the lifted end had fully emerged from the water. All sheets had a width b of 0.80 m and an initial length ℓ of 4.40 m.

From the results listed in Table 2, it can be seen that the calculated values for σ_b given by the three methods are very consistent and remain within ten percent of an average value of $10.9 \times 10^5 \text{ N/m}^2$. On the other hand, the x-F method gives usually larger values of E than either the y-F or the x-y method, both of which predict E values nearly equal. The y-F method predicts an average value for E of $(1.74 \pm 0.35) \times 10^9 \text{ N/m}^2$, the x-y method a value of $(2.06 \pm 0.37) \times 10^9 \text{ N/m}^2$, and the x-F method a value of $(4.0 \pm 1.9) \times 10^9 \text{ N/m}^2$. Since E is proportional to L^4 , relatively small discrepancies in the calculated value of L lead to large variations in E . As can be seen from figure 6, in the neighborhood of $F^* = 1$, small changes in F^* correspond to large variations in x_o/L and y_o/H , and therefore in L ; for example, as F^* varies from 0.95 to 1.0, a change of only five percent, x_o/L varies from 0.6 to 1.0, a forty percent change, and y_o/H varies from 2.1 to 3.8, an eighty percent change. To illustrate further the above remarks, let us consider experiment F-1. With the given values of h , F and x_f , F^* is calculated to be 0.989, and the corresponding values of L and E are 0.77 m and $4.6 \times 10^9 \text{ N/m}^2$, respectively. However, x_f can be measured at best within one centimeter, since the break in the ice sheet is never perfectly straight, and x_f represents an average floe length over the width of the ice sheet. F^* could have been taken equal to 1.0, just as well; the corresponding values for L and E would have been, $L = 0.69 \text{ m}$ and $E = 3.0 \times 10^9 \text{ N/m}^2$.

Table 2. Calculation of Ice Mechanical Properties - Initial Experiments

Exp #	Experimental Data						Y-F Method				Analyses Results X-Y Method				X-F Method				
	h	y _{of}	F _f	x _f	L	x _O	E	σ_b^2	x _f	L	x _O	E	σ_b^2	F _f	L	x _O	E	σ_b^2	y _{O_f}
	mm	mm	N	cm	cm	cm	N/m ² x10 ⁻⁹	N/m ² x10 ⁻⁵	cm	cm	cm	N/m ² x10 ⁻⁹	N/m ² x10 ⁻⁵	N	cm	cm	N/m ² x10 ⁻⁹	N/m ² x10 ⁻⁵	mm
F-1	13	81	65	70	58	81	1.50	10.0	69	58.5	81.5	1.57	10.2	66	77	62	4.6	10.0	22
F-2	19	73	110	90	78	82	1.58	9.2	80	87.5	92.5	2.51	11.5	123	111	50	6.5	9.4	30
F-3	22	89	160	100	96	105	2.37	12.5	101	95.5	104.5	2.30	12.3	159	100	100	2.76	12.3	78
F-4	25	85	178	100	100	97	1.87	10.5	99	101.2	98.7	1.98	10.8	180	111	87	2.82	10.5	64
F-5	29	110	222	120	103	109	1.38	10.5	106	117	123	2.27	13.4	251	148	64	5.83	10.8	45
F-6	38	95	325	120	134	103	1.73	11.2	120	134	103	1.71	11.1	324	132	105	1.64	10.0	98

In conclusion to the above discussions, it is suggested that the x-F method be used to determine the elastic modulus index E only when the quantity F^* is less than 0.85 to 0.90. For values of F^* greater than 0.85, the y-x and y-F methods are to be preferred, even though it is likely that x_f and F_f are more easily measured than y_{of} . All three methods can be used to obtain reliable estimates of the strength index σ_b .

D. Experiments with Sloping Planes

In the second experimental phase of the study, a sloping structure was mounted in the tank. Its slope could be varied from 10° to 80° . This structure, constructed of aluminum angles, spanned the entire width of the tank and was instrumented with two moment insensitive dynamometers to measure the horizontal and vertical force, F and P exerted by an ice sheet pushed at constant speed against it. A sketch and photograph of the instrumented sloping plane are shown in Figures 10 and 11, respectively.

Five experiments were conducted, three with the plane inclined at $\theta = 37^\circ$, and two at $\theta = 45^\circ$. In each test, continuous records of the forces F and P were obtained from which the failure forces F_f and P_f , and the time of failure t_f were measured. In addition the length of the broken floe was also measured.

Since the ice sheets used in these experiments were grown in the same way as those tested in the first experimental phase, the value of σ_b adopted in the prediction of F_f and P_f was the average of all values listed in Table 1, while that of E was the average of the values of E in Table 1 predicted by the Y-F and X-Y method, namely

$$\begin{aligned}\sigma_b &= 10.9 \times 10^5 \text{ N/m}^2 \\ E &= 1.9 \times 10^9 \text{ N/m}^2\end{aligned}$$

The theory developed earlier for the conditions $P = 0$, $M_o = 0$, $F \neq 0$, was applied to predict the value of F_f , the corresponding value of P_f was then calculated as

$$P_f = F_f \tan \theta$$

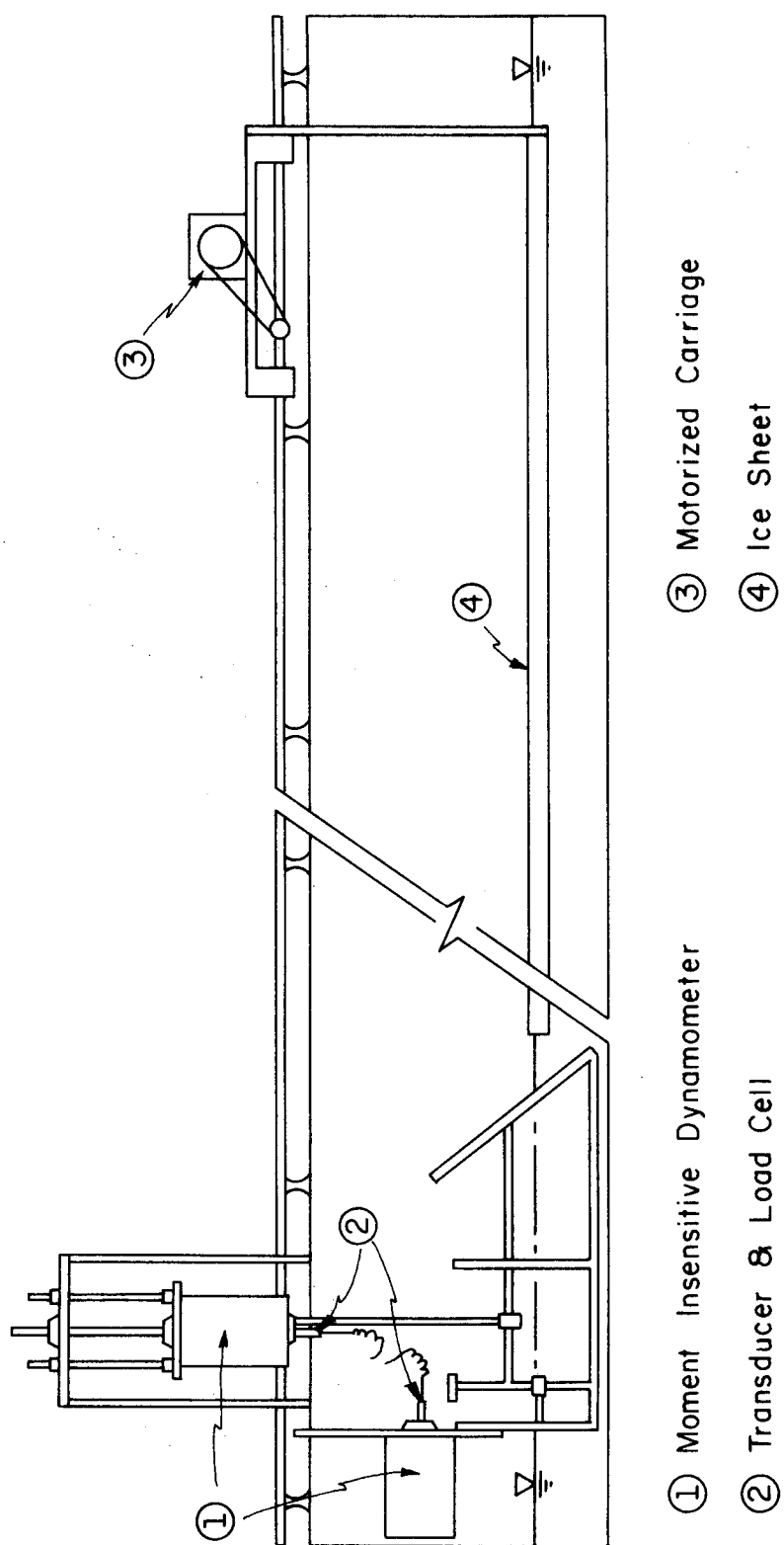
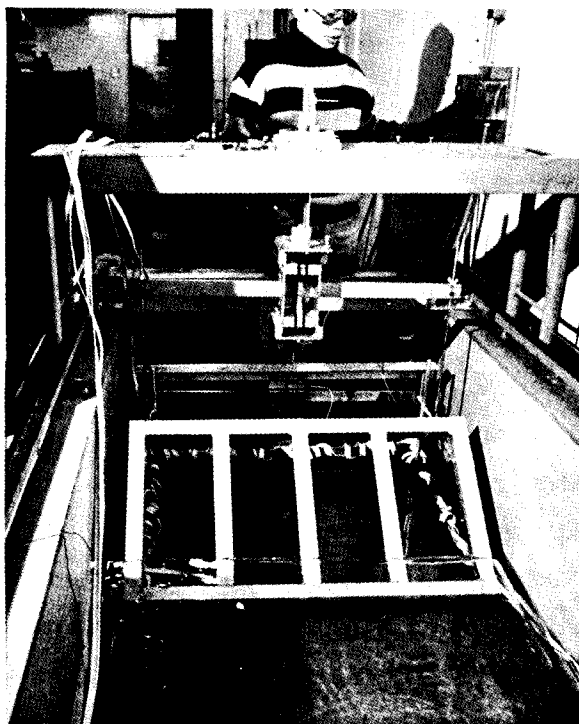
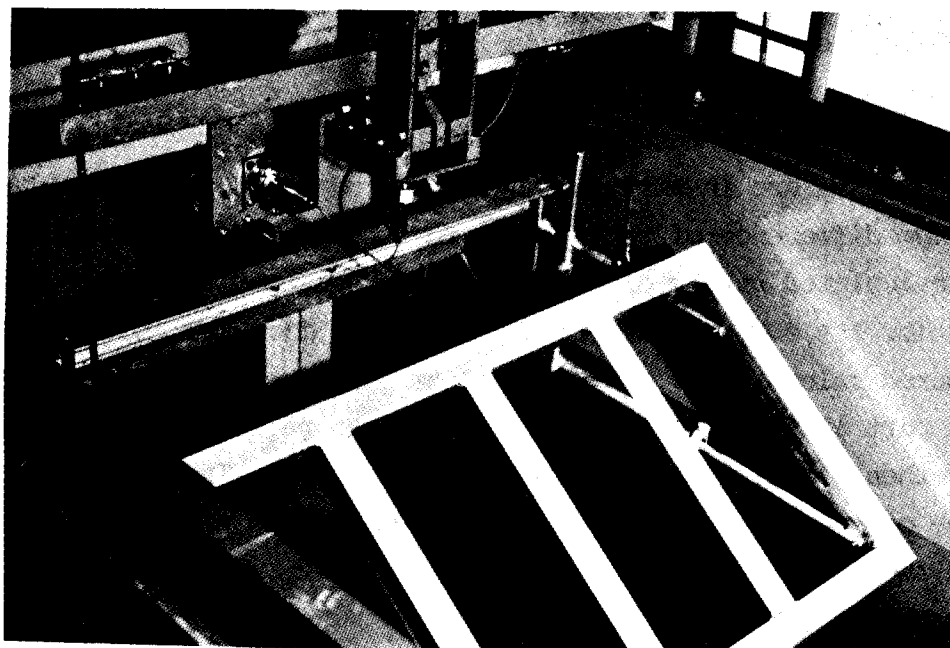


Figure 10. Sketch of Experimental Sloping Plane



Apparatus in operation



Close-up view

Figure 11. Photographs of Experimental Sloping Plane

that is that the friction factor μ between ice and structure was assumed to be zero. This approximation was based on the fact that, by construction of the experimental structure, the ice sheet was supported by only five smooth, narrow aluminum angles, as can be observed on Figure 11. Also the angle θ could be measured at best within an accuracy of one degree, and therefore $\tan \theta$, for $\theta = 37^\circ$ or 45° , was known within an accuracy of ± 4 percent. Finally repeated calibration of the force measuring systems indicated an accuracy in the measured values of F_f and P_f of approximately 5 percent.

The experimental data and the predicted values of F_f , P_f , and x_f are listed in Table 3. All the ice sheets were thin enough for the riding edge to emerge from the water since, the minimum thickness for the sheet not to emerge is

$$h = 3.2 \left(\frac{\rho_w}{\rho_i} \right)^2 \frac{\sigma_b^2}{\gamma_w E} = 0.24 \text{ m}$$

which is one order of magnitude larger than the thickness of the experimental ice sheets.

From the results of Table 3, it can be seen that the predicted values of F_f are in very good agreement with its measured values with a maximum difference of ten percent for the last and thickest ice sheet. The calculated values of P_f are in good agreement with the measured ones for $\theta = 45^\circ$, but are twenty to twenty five percent smaller than the measured values for $\theta = 37^\circ$. Besides experimental errors, it is likely that part of the discrepancy is due to the neglect of friction. For $\theta = 37^\circ$, then $\phi = 0.75$ if μ is assumed to be zero. The average measured value of ϕ for $\theta = 37^\circ$ is 0.97 corresponding to a value of $\mu = 0.13$. With the latter value of μ , the calculated P_f would fall within five percent of the measured one.

E. Experimental Determination of σ_b and E for Urea-Doped Ice

Timco (1980) proposed that urea-doped ice be used instead of saline ice as model ice in laboratory modeling of ice-structure interaction such as ice breakers model studies. The results of his experiments

Table 3. Results of Experiments with Sloping Planes

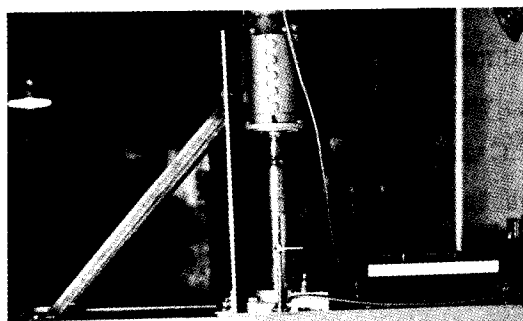
Run #	θ (°)	U_o mm/s	Experimental Data				Calculated Values ($\mu = 0$)						
			h mm	F_f N_f	P_f N_f	x_f cm	ϕ	t_f (sec)	F_f N_f	P_f N_f	x_f cm	y_{of} mm	y_{of}
-1	45	1.67	13	65	67	70	1.03	35	68	68	72	74	56
-2	45	3.33	16	89	89	90	1.00	18	93	93	80	77	60
-3	37	1.67	19	113	113	90	1.00	52	120	90	87	79	87
-4	37	3.33	22	147	147	90	1.00	26	149	112	94	82	87
-5	37	3.33	32	291	267	120	0.92	30	262	197	113	89	100

on urea-doped ice indicate that the ratio E/σ_b remains equal to or larger than 2000 for a flexural strength σ_b as low as 20 kpa, for ice grown from a 1.3% solution of carbamide (urea) in water. These values of the mechanical properties of the model ice would allow a model scale up to $\lambda = 50$, while the maximum value of λ is of the order of 20 when saline ice is used as model material. In Timco's experiments, the strain modulus E was measured by the plate method, and the flexural strength σ_b was measured by the cantilever beams method, with the beams loaded downward.

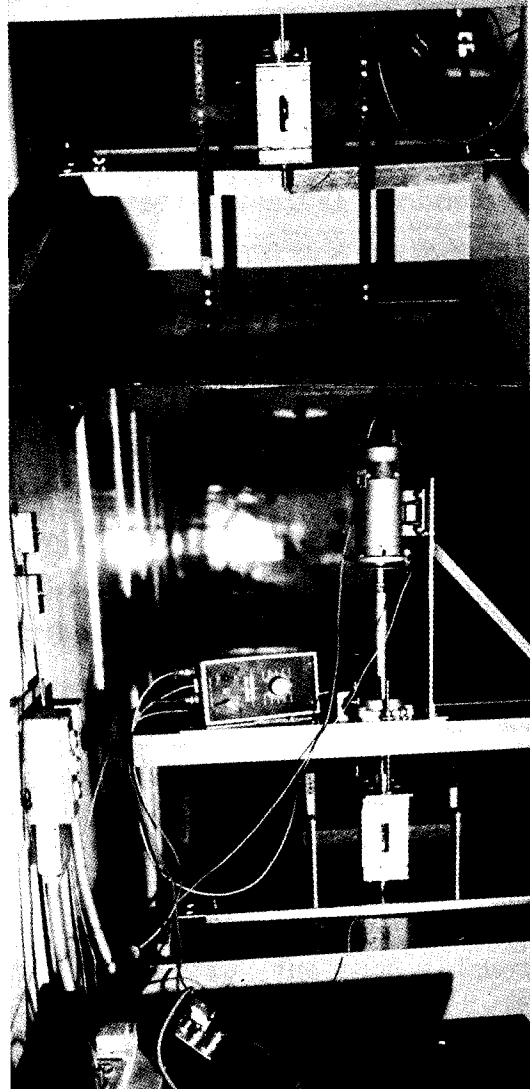
It was then decided to determine the mechanical properties of urea-doped ice by the method of the floating ice sheet described in section VI-C above and previously applied to freshwater ice sheets. A first series of experiments was conducted with the lift-push apparatus used in the freshwater ice experiments. This apparatus permitted to achieve a maximum vertical speed of approximately 3.5 mm/sec. Because of concern that at large urea concentration the rate of deformation might not be high enough to insure elastic deformation of the ice, the apparatus was later modified by eliminating the right-angle speed reducer and connecting the motor shaft directly to the threaded rod supporting the instrumented lift-push device. The maximum vertical speed was then increased to about 30 mm/sec. A photograph of the direct drive lift-push apparatus is shown in Figure 12.

The experimental program was designed to investigate the effect of initial urea concentration in the water bath, test temperature, and load direction (push or lift). The tests performed so far have all been conducted in the lift mode, and only three urea concentrations have been tested, namely 0.3, 0.6 and 0.75%. Therefore the results presented in Table 4 are to be considered as preliminary. The general experimental procedure was as follows.

1. The air temperature was brought to about -7.5°C and the water bath, except for the first sheet tested, was constantly circulated in order to achieve a homogeneous temperature throughout. When the initial ice layer formed naturally at the water surface, the layer was skimmed off and the bath was wet seeded by spraying a fine mist above the tank. The resulting ice crystals formed in the air deposited at the surface of the water and initiated the test ice sheet. The ice sheet was grown for twenty four to thirty six hours to reach a thickness of several centimeters.



Front View



Back View

Figure 12. Photograph of Direct Drive Lift-Push Apparatus

2. Once the ice sheet had reached the desired thickness it was either tested immediately at a room temperature of -7.5°C , or the refrigerated system was turned off and the room temperature let to rise slowly to about -1°C at which time the tests were conducted. The warm up time varied from twelve to eighteen hours.

No thin sections of the ice were made to examine its structural features; however, it was observed that the urea ice was quite unhomogeneous with a hard, thin top layer very similar to freshwater ice, and a thicker, mushy bottom layer similar to saline ice. Overall, urea ice appeared to be more "porous" than saline ice; when removed from the melt, an ice sample would be drained very rapidly of its liquid constituent. Also, freeboard observations indicated that urea ice is denser than both freshwater and saline ice in agreement with Timco's observations. This latter feature became apparent for urea concentration of 0.5% and larger.

The experimental records of lift-force versus time often showed the force increasing then leveling off with no sudden drop, which, in the case of freshwater ice, was indicative of failure. However, a line of fracture across the ice sheet could be observed to form approximately at the time the lift force started to level off. Because of this feature, the displacement y_{o_f} of the free end at failure could not be determined with certainty. It was then decided that σ_b and E would be determined by the X-F method, taking F_f as the maximum force recorded and x_f the length of the broken floe.

The experimental data and the results of the computations are shown in Table 4. It can be observed that σ_b decreases slowly with increasing urea concentration, is only slightly affected by the air temperature, and that its values for nominally identical experimental conditions remain reasonably constant, with maximum deviation of about 50%. On the other hand, the calculated values of E can vary widely between experiments conducted under the same nominal conditions. It can also be noted that for the same urea concentration and air temperature, the thinner ice sheets yield larger values of both σ_b and E (for example, ice sheets #5 and 6 or 7). It can be conjectured that most of the strength and stiffness of the ice sheet arises from the top layer which occupies a larger percentage of the total ice thickness for thin ice sheets.

As mentioned previously, the experiments with urea doped ice are still underway, and more comprehensive results will be available when the experimental program is completed.

Table 4. Results of Experiments with Urea-Doped Ice

Sheet #	Urea Concentration %				Experimental Data							Calculated Quantities (X-F Method)			
	Water	Ice	Average	Top Ice	Bottom Ice	b cm	T _A °C	h mm	H mm	n ₀ mm/s	H ₀ mm	n ₀ mm/s	H ₀ mm	H ₀ mm	H ₀ mm
1	0.31	0.04			40	-1		32	29.4	0.8	87	121	650	5100	8000
2	0.36	0.03						28	25.8	0.8	79	116	750	6400	8500
								25.4	23.4	3.4	65	87	270	2640	9800
3	0.38	0.10	0.05	0.16	79	-0.5		20.6	18.9	3.4	58	111	470	13000	27700
								41.3	38	3.3	84	46	71	49	690
4	0.4	0.13	0.08	0.13	79	-7.5		41.3	38	3.4	76	46	64	49	766
								37.3	34.3	3.4	47	63	66	235	3500
4	0.4	0.13	0.08	0.13	79	-7.5		36.5	33.6	3.2	60	84	118	792	6700
								26.2	24.1	3.5	48	53	120	340	2800
4	0.4	0.13	0.08	0.13	79	-7.5		24.4	22.5	3.2	43	38	85	111	1300
								23.8	21.9	3.4	57	34	128	43	340
4	0.4	0.13	0.08	0.13	79	-7.5		22.6	20.8	3.2	57	49	173	385	2200

Table 4 (Cont'd). Results of Experiments with Urea-Doped Ice

Urea Concentration %				Experimental Data				Calculated Quantities (X-F Method)						
Sheet #	Water	Ice Average	Top Ice Layer	Bottom Ice Layer	b cm	T _A °C	h mm	H mm	ρ ₀ mm/s	N _H mm/s	x _m mm	ρ ₀ kg/m ³	E MPa	E/ρ ₀
5	0.58				30	-1	27	25.7	0.83	20	63	140	620	4400
							27	25.7	1.33	19	45	100	160	1600
							25	23.8	1.9	16	39	80	120	1500
							25	23.8	1.9	17	48	110	260	2400
6	0.58	0.20	0.14	0.23	80	-7.5	55	52.3	1.23	107	64	70	78	1100
							54	51.3	3.4	102	59	64	60	940
							53	50.4	3.4	94	51	52	35	670
							52	49.4	3.3	120	45	62	23	370
7	0.58	0.23			80	-7.5	28	26.6	3.4	54	38	83	76	920
							25.4	24.1	3.5	52	41	100	130	1300
							24.4	23.2	3.2	45	34	81	73	900
							29.3	27.8	3.5	56	31	67	24	360

Table 4 (Con't). Results of Experiments with Urea-Doped Ice	Calculated Quantities
---	-----------------------

Sheet #	Urea Concentration %						Experimental Data							(X-F Method)		
	Water	Average Ice	Top Ice Layer	Bottom Ice Layer	b _{cm}	T _A °C	p _{mm}	H _{mm}	ρ _{g/cm³}	N _H %	X _F %	G _g	Q _g	K _P	M _P	E _H /E _a
8	0.53	0.20	0.11	0.29	79	-1.0	31	29.5	4.3	58	52	98	190	190	190	1900
							28.4	27.0	4.3	60	53	123	266	266	266	2200
							33	31.4	4.3	64	55	100	197	197	197	2000
							33	31.4	4.3	51	37	54	40	40	40	740
9	0.53	0.13	0.06	0.21	79	-0.5	28	26.6	4.3	70	46	132	156	156	156	1200
							25.4	22.8	4.3	60	49	141	266	266	266	1900
							22.8	21.7	4.1	58	52	180	469	469	469	2600
10	.55	0.19	0.07	0.20	79	-0.5	28.4	27.0	4.3	73	52	146	244	244	244	1700
							26	24.7	4.3	60	34	104	44	44	44	420
							26	24.7	4.3	46	34	72	55	55	55	760
							26	24.7	4.3	58	35	102	61	61	61	600
11	0.60				91	-0.5	30	28	3.3	75	50	113	179	179	179	1600
							27.7	26.3	3.4	78	56	153	353	353	353	2300

VII. SUMMARY AND CONCLUSIONS

Under the assumption that ice is a homogeneous, elastic material, analytical expression for the horizontal and vertical forces exerted by an ice sheet on a two-dimensional sloping plane have been derived. It has been shown that an ice sheet of length three times or more a characteristic length L , defined as $(Eh^3/3\gamma_w)^{\frac{1}{4}}$, can be considered as semi-infinite. Also the analytical results indicate that the horizontal force and bending moment at the frontal edge of the ice sheet have little influence on the deformation of the ice sheet. The ice sheet can then be treated, for practical application, as subjected only to a vertical force. The resulting analysis and final expressions for the maximum force exerted on the sloping plane are considerably simplified without significant loss in accuracy.

Two critical ice thicknesses have been identified, h_{\min} and h_{\max} . They have been expressed in terms of the mechanical properties σ_b and E of the ice, and its specific gravity, and have been shown to depend on the direction of application, upward or downward, of the vertical force F exerted at the frontal edge of the ice sheet. When the ice thickness is larger than h_{\max} , the failure force F_f is proportional to σ_b , inversely proportional to $E^{\frac{1}{4}}$, and proportional to $h^{\frac{5}{4}}$. When the ice thickness is less than h_{\min} , F_f is proportional to $\sigma_b^{\frac{1}{2}}$ and to $h^{\frac{3}{2}}$, but independent of E . This latter result has the important consequence that in model studies of ice forces on inclined structures, where the condition $h < h_{\min}$ is satisfied, only the bending strength σ_b of the ice need be properly scaled, while the elastic modulus of the model ice may take any value, as long as the model ice behaves as an elastic material.

The analytical expressions have been verified satisfactorily in experiments conducted with freshwater ice sheets. An experimental program has been initiated, where the analytical expressions are used in the determination of the mechanical properties of urea-doped ice. Only preliminary results of this experimental program, which is still underway, have been presented.

It remains to be verified, either analytically or experimentally, that the main results obtained here remain valid for the case of ice forces on three-dimensional structures such as sloping planes of finite span and conical structures. In particular if there exists a critical ice thickness below

which the maximum ice force is independent of the ice elastic modulus, model studies could be performed without concern about the elastic modulus of the model ice.

VIII. REFERENCES

- Frederking, R., (1979), "Dynamic Ice Forces on an Inclined Structure," IUTAM Symposium, Copenhagen 1979, Physics and Mechanics of Ice, P. Tryde Editor, Springer-Verlag, Berlin.
- Michel, B., (1978), "Ice Mechanics," Les Presses de L'Universite Laval, Quebec.
- Nevel, D.E. (1979), "Bending and Buckling of a Wedge on an Elastic Foundation," IUTAM Symposium, Copenhagen 1979, Physics and Mechanics of Ice, P. Tryde Editor, Springer-Verlag, Verlin.
- Pounder, E.R., (1965), "The Physics of Ice," Pergamon Press, New York.
- Ralston, T.D., (1979), "Plastic Limit Analysis of Sheet Ice Loads on Conical Structures," IUTAM Symposium, Copenhagen 1979, Physics and Mechanics of Ice, P. Tryde Editor, Springer-Verlag, Berlin.
- Sørensen, C., (1978), "Interaction Between Floating Ice Sheets and Sloping Structures," Institute of Hydrodynamics and Hydraulic Engineering, Technical University of Denmark, Series Paper No. 19.
- Tatinclaux, J.C. and Wu, C.Y., (1976), "Laboratory Study of the Flexural Strength and Elastic Modulus of Freshwater and Saline Ice," IIHR Report No. 180, Iowa Institute of Hydraulic Research, University of Iowa, Iowa City, Iowa.
- Timoshenko and Young, (1968), Elements of Strength of Materials/5th Edition, D. Van Nostrand Company, Inc., Princeton, New Jersey.
- Tryde, P., (1972), "A Method of Predicting Ice Pillings Impact of Floe Against Inclined Plane," Tech. Univ. of Denmark, Progress Report No. 26.
- Weeks, W.F., and Assur, A., (1969), "Fracture of Lake and Sea Ice," Report RR-269, U.S. CRREL, Hanover, New Hampshire.